Study of Cloud-Driven Multi-Way Multiple-Antenna Relay Systems with User Selection and Joint Detection

F. L. Duarte and R. C. de Lamare, *Senior Member, IEEE*

***Abstract*—In this work, we present a cloud-driven uplink framework for multi-way multiple-antenna relay systems which aids joint symbol detection in the cloud and where users are selected to simultaneously transmit to each other aided by relays. We also investigate relay selection techniques for the proposed cloud-driven uplink framework that uses cloud-based buffers and XOR network coding. In particular, we develop a novel multi-way relay selection protocol based on the selection of the best link, denoted as Multi-Way Cloud-Driven Best-User-Link (MWC-Best-User-Link). We then devise maximum-minimum-distance and channel-norm based relay selection criteria along with algorithms that are incorporated into the proposed MWC-Best-User-Link protocol. An analysis of the proposed MWC-Best-User-Link protocol in terms of computational cost, pairwise error probability, sum-rate and average delay is carried out. Simulations show that MWC-Best-User-Link outperforms previous works in terms of sum-rate, pairwise error probability, average delay and bit error rate.**

***Index Terms*—Multi-Way Relay Channel, Cooperative diversity, Maximum Likelihood detection, Minimum Mean Square Error detection, MIMO**

I. Introduction

In wireless networks, the use of cooperative diversity[1], [2] can mitigate the signal fading caused by multipath propagation. The Multi-Way Relay Channel (mRC) [3] includes both a full data exchange model, in which each user receives data from all other users, and the pairwise data exchange model, which is composed by multiple two-way relay channels. The incorporation of the mRC with multiple relays in a system can significantly improve its performance [4], [5], [6], [7]. Considering 5G requirements [8], high spectrum efficiency relaying strategies are key due to their excellent performance. The use of a cloud as a central node can leverage the performance of relay techniques as network operations and services have recently adopted cloud-enabled solutions in communication networks [9], [10]. The ability to manage interference is one of the main advantages of adopting the cloud network framework [10]. In the Cloud Radio Access Network (C-RAN) architecture, the baseband processing, usually performed locally at each base-station (BS), is aggregated and performed centrally at a cloud processor. This is enabled by high-speed connections, denoted as fronthaul links, between the BSs and the cloud [10]. This centralized signal processing enables the interference mitigation across all the users in the uplink and downlink. The BSs in the C-RAN are also referred to as remote radio heads (RRHs) as their functionality is often limited to transmission and reception of radio signals [10]. These RRHs are driven by the cloud-processor that communicates with RRHs via fronthaul links, that can be dedicated fiber optic cables or wireless links [10]. From an information theoretical point of view, the C-RAN model is best understood as a relay network [10], in which the RRHs can be considered as relays that cooperate in the communication between the cloud and the mobile users. In the uplink, different users in the same cluster communicate their messages to the cloud through RRHs (relays). The relays, instead of decoding the messages locally, can retransmit information about their received signals to the cloud for centralized processing [10]. The uplink in the C-RAN can thus be modeled as a multiple-access relay channel [10]. Moreover, in the downlink, the cloud also communicates with multiple users through RRHs and the downlink in the C-RAN can thus be modeled as a broadcast relay channel [10].

A. Prior and Related Work

The mRC has multiple clusters of users in which each user aims to multicast a single message to all the other users in the same cluster [3]. Considering $\mathcal{L}$ users in a cluster corresponds to an $\mathcal{L}$-way information exchange among the users in the same cluster. A group of N relays facilitates this exchange, by helping all the users in the system. In particular, the mRC pairwise data exchange model ($\mathcal{L} = 2$) is formed by multiple two-way relay channels. In Two-Way Multiple-Access Broadcast Channel (MABC) schemes, based on the decode-and-forward (DF) protocol [11], the transmission is organized in two successive phases: 1) MA phase - a relay is selected for receiving and decoding the messages simultaneously transmitted from two users (sources S_1 and S_2) and physical-layer network coding (PLNC) is performed on the decoded messages; 2) BC phase - the same selected relay broadcasts the decoded messages to the two sources. The Two-Way Max-Min (TW-Max-Min) relay selection protocol [11] has a high performance, when all the channels are reciprocal and fixed during two consecutive time slots (MA and BC phases). Otherwise, with non reciprocal channels, the performance of relaying strategies can be enhanced by adopting buffer-aided protocols, in which the relays are able to accumulate data in their buffers [12], [14], [13], before sending data to the destination, as in the MW-Max-Link [15] protocol for cooperative multi-input multi-output (MIMO) systems, which selects the best links among K pairs of sources (diversity gain

F. L. Duarte is with the Centre for Telecommunications Studies (CETUC), Pontifical Catholic University of Rio de Janeiro, Brazil, and the Military Institute of Engineering, IME, Rio de Janeiro, RJ, Brazil. e-mail: flaviold@cetuc.puc-rio.br

R. C. de Lamare is with the Centre for Telecommunications Studies (CETUC), Pontifical Catholic University of Rio de Janeiro, Brazil, and the Department of Eletronic Engineering, University of York, United Kingdon. e-mail: delamare@cetuc.puc-rio.br

equals $2NK$), using the extended Maximum Minimum Distance (MMD) relay selection criterion [16], [17]. Furthermore, in [18], the TW-Max-Link protocol (a special case of MW-Max-Link, for a single two-way relay channel ($K = 1$)), also using the extended MMD criterion, was presented. Some other buffer-aided relay selection protocols for cooperative single-antenna and multiple-antenna systems are presented in [19], [20], [21], [22], [23], [24], [25], [26], [27]. Moreover, sum-rate maximization is reported for relay selection using two-way protocols, with single-antenna systems in [28]. However, multi-way protocols using a channel-norm based criterion for sum-rate maximization, with multiple-antenna systems, or a cloud (in which each cluster has a particular buffer), have not been previously investigated.

B. Contributions

In this work, we develop a cloud-driven framework and a Multi-Way Best-User-Link (MWC-Best-User-Link) protocol for cooperative MIMO systems, with non reciprocal channels, which selects the best links among K pairs of sources (clusters) and N relay nodes and whose results were reported in [16], [82]. In order to perform signal detection at the cloud and the nodes, we present maximum likelihood (ML) and linear minimum mean-square error (MMSE) detectors. We then consider the extended Maximum Minimum Distance (MMD) [16], [17] criterion and a channel-norm based (CNB) criterion and devise relay selection algorithms for MWC-Best-User-Link. An analysis of the proposed scheme in terms of pairwise error probability (PEP), sum-rate, average delay and computational cost is also carried out. Simulations illustrate the excellent performance of the proposed framework, the proposed MWC-Best-User-Link protocol and the relay selection algorithms as compared to previously reported approaches. Therefore, the main contributions of this work are:

1) A cloud-driven framework with joint detection at the cloud and the nodes;
2) The MWC-Best-User-Link multi-way protocol for cooperative MIMO systems;
3) The MMD and CNB relay selection criteria along with relay selection algorithms;
4) An analysis of the proposed MWC-Best-User-Link scheme in terms of PEP, sum-rate, average delay and computational cost.

This paper is structured as follows. Section II describes the system model and the main assumptions. Section III presents the proposed MWC-Best-User-Link protocol, relay selection criteria and algorithms. Section IV analyzes MWC-Best-User-Link, with the extended MMD and the novel low-complexity CNB criteria for relay selection. Section V illustrates and discusses the simulation results whereas Section VI gives the concluding remarks.

II. System Description

We assume a MIMO multi-way MABC relay network formed by K clusters (pair of sources S_1 and S_2) and N half duplex (HD) DF relays, R_1,...,R_N. In a C-RAN, the sources would represent mobile users and the relays would represent RRHs. The sources have M_S antennas for transmission or reception and each relay $M_R = 2UM_S$ antennas, where $U \in \{1, 2, 3 \dots\}$, all of them used by the selected relay for reception ($M_{R_{rx}} = M_R$) and M_S out of VM_S antennas are selected of each relay used for transmission ($M_{R_{tx}} = M_S$), where $V \in \{1, 2, 3 \dots\}$ and $VM_s \leq M_R$, forming a spatial multiplexing network, in which the channel matrices are square or formed by multiple square sub-matrices in the MA mode. Note that the reason for using multiples of $2M_S$ antennas at the relays is because the relay selection algorithms explained in Section III use criteria that depend on these matrices to be square or to be formed by multiple square sub-matrices. Thus, the higher V the better the system performance, as it increases the degrees of freedom. Moreover, the higher U the better the system performance as it increases the number of receive antennas at the relays. However if we increase U and V, we have a higher computational complexity, as shown in Section IV. There is a trade-off between system performance and computational complexity, when we increase U and V. The selected relays access a number of K cloud buffers for extracting or storing M_S packets in each time slot. Each cluster has a particular cloud buffer that is established on demand, whose size is J packets, as depicted in Fig.1. In the multiple-access phase (uplink), a cluster is selected to send M_S packets simultaneously to a selected relay R_g for reception. Then, the data is decoded by the cloud processor and XOR type PLNC [29], [18], [15] is applied to combine the decoded vectors (inputs of the XOR) and generate a codeword (output of the XOR) that is stored in their particular cloud buffers. In the broadcast-channel phase (downlink), two relays R_{f1} and R_{f2} are selected to broadcast M_S packets from the particular cloud buffer to the selected cluster. Note that R_{f2} may be different from R_{f1}. In most situations the selection of only one relay in the downlink is enough for a good performance. However, by selecting two relays, the possibility of combining the channels related to the selected relays increases the degrees of freedom of the system and, consequently, its performance is improved. The system could select more than two relays to further improve its performance, but the computational complexity would be considerably increased for a high number of relays. For simplicity, we adopt the mRC pairwise data exchange model, but the full data exchange model can be considered in future works. Moreover, other kinds of network coding, as linear PLNC [14] and analog network coding [30], can be considered in future works.

A. Assumptions

We assume a non prefixed schedule protocol, in which each time slot may be selected for uplink or downlink transmission, depending on the quality of the available links and the buffer status. Thus, the energy transmitted from each source node to the selected relay for reception (E_S) or from the selected relay(s) for transmission to the sources (E_{R_f}), in each time slot, is the same, i. e., $E_{R_f} = E_S$. The use of power allocation ($E_{R_f} \neq E_S$) would imply a more complex relay selection algorithm, but can be considered elesewhere in future works with prefixed schedule protocols, using precoders that rely

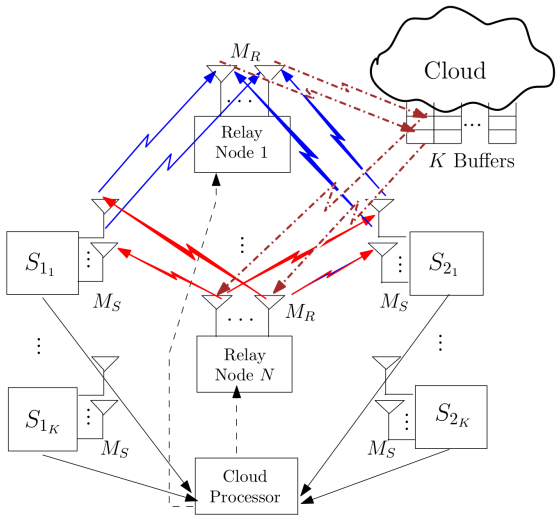

Fig. 1. System model of the proposed cloud-driven multi-way relay scheme.

on CSI (in practice imperfect CSI) at the transmitters. We consider mutually independent zero mean complex Gaussian random channel coefficients, which are fixed for the duration of one time slot and vary independently from one time slot to the following, and the transmission is organized in data packets. Fig. 2 illustrates the frame of the data packets. The order of the packets is contained in the preamble and the original order is recovered at the destination. Signaling for network coordination and pilot symbols for estimation of the channel state information (CSI) are also contained in the preamble. The cloud is the central node and decides whether a cluster or the relay(s) must transmit in a given time slot i, through a feedback channel. An appropriate signalling provides global CSI at the cloud [12]. Moreover, we assume that each relay only has information about its S_1R and S_2R links. The use of a cloud as a single central node and its buffers implies a higher control overhead. However, it reduces the system complexity and the delay, since a unique central node decides which nodes transmit (rather than all destination nodes) and the packets associated with a cluster are stored in only its particular cloud buffer instead of being spread in the buffers of all relays. In this work, we focus on the ideal case where the fronthaul links have unconstrained capacities, and the relays can convey their exact received signals to the cloud processor. This could happen only if the relays were near to the cloud and experiencing high signal-to-noise and low interference conditions. Practical systems, however, have capacity-constrained fronthaul links [10] and this limits the amount of information that the relays can retransmit. Although these unconstrained capacities in the fronthaul links simplify our analysis, they do not limit the advantages of the proposed protocol and relay selection algorithms, explained in the next section. In this context, it is worth noting that 5G systems are designed to achieve very high fronthaul links capacity, and thus, the considered unconstrained capacity assumption is reasonable for the purpose of the relay and cloud communication. Moreover, capacity-constrained fronthaul links can be considered elsewhere in future works and the performance achieved by the proposed protocol may be considered as an upper bound.

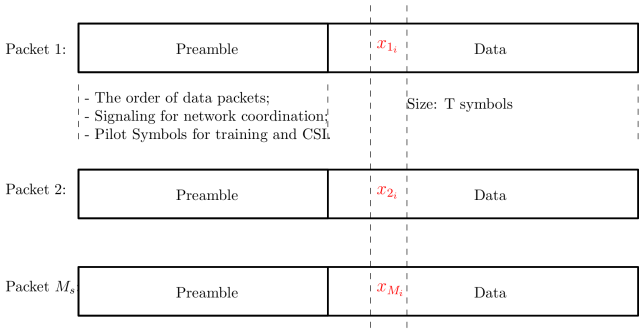

Fig. 2. The frame of each packet.

B. System Model

The wireless channel matrix $\mathbf{H}_{S_k,R_i}$ incorporates the effects of large-scale fading, related to the propagation characteristics of the signal over long distances, and the Rayleigh-distributed small-scale fading [31]. Hence, the quadratic norm of $\mathbf{H}_{S_k,R_i}$ is given by

$$\|\mathbf{H}_{S_k,R_i}\|^2 = \gamma \; d_{S_k,R_i}^{-2\xi} \, \|\mathbf{G}_{S_k,R_i}\|^2 \tag{1}$$

where S_k represents each source S_{1_k} or S_{2_k} ($k \in \{1 \dots K\}$), R_i represents each relay ($i \in \{1 \dots N\}$), γ represents a constant defined by the antenna gain, carrier frequency and other system parameters, ξ is the path-loss component, $\mathbf{G}_{S_k,R_i}$ represents a channel matrix related to the S_kR_i links formed by mutually independent zero mean complex Gaussian random coefficients and d_{S_k,R_i} the respective distance between S_k and R_i. The same reasoning applies to $\mathbf{H}_{R_i,S_k}$ and its quadratic norm is given by

$$\|\mathbf{H}_{R_i,S_k}\|^2 = \gamma \; d_{R_i,S_k}^{-2\xi} \, \|\mathbf{G}_{R_i,S_k}\|^2 . \tag{2}$$

The proposed system can operate in each time slot in two modes: "Multiple-Access" (MA) or "Broadcast-Channel" (BC). Thus, depending on the relay selection metrics (explained in Section III), the system may operate in each time slot with two options:

a) MA mode: The selected cluster transmits M_S packets directly to the selected relay R_g;

b) BC mode: R_{f1} and R_{f2} transmits M_S packets from the cloud buffers to the selected cluster.

If the relay selection algorithm decides to operate in the MA mode, the signal sent by the selected cluster S (S_1 and S_2) and received at R_g (the relay selected for reception) is organized in an $2UM_S \times 1$ vector given by

$$\mathbf{y}_{S,R_g}[i] = \sqrt{\frac{E_S}{M_S}} \mathbf{H}_{S,R_g} \mathbf{x}[i] + \mathbf{n}_{R_g}[i], \tag{3}$$

where $\mathbf{x}[i]$ is an $2M_S \times 1$ vector with M_S symbols sent by S_1 ($\mathbf{x_1}[i]$) and S_2 ($\mathbf{x_2}[i]$), $\mathbf{H}_{S,R_g}$ is a $2UM_S \times 2M_S$ matrix of S_1R_g and S_2R_g links and $\mathbf{n}_{R_g}$ is the zero mean additive white complex Gaussian noise (AWGN) at R_g. Note that $\mathbf{H}_{S,R_g}$ is

formed by U square sub-matrices of dimensions $2M_S \times 2M_S$ as given by

$$\mathbf{H}_{S,R_g} = [\mathbf{H}^1_{S,R_g}; \mathbf{H}^2_{S,R_g}; \dots ; \mathbf{H}^U_{S,R_g}]. \quad (4)$$

Assuming perfect synchronization, we may adopt the ML receiver at the cloud processor:

$$\hat{\mathbf{x}}[i] = \arg\min_{\mathbf{x}'[i]} \left(\left\| \mathbf{y}_{S,R_g}[i] - \sqrt{\frac{E_S}{M_S}} \mathbf{H}_{S,R_g} \mathbf{x}'[i] \right\|^2 \right), \quad (5)$$

where $\mathbf{x}'[i]$ is each of the $N_s^{2M_S}$ possible vectors of sent symbols (N_s is the quantity of symbols in the constellation adopted). The ML receiver calculates an estimate of the vector of symbols sent by the sources $\hat{\mathbf{x}}[i]$.

In contrast, by considering linear MMSE detection [32], the estimate of the transmitted vectors $\mathbf{x}$ is obtained by processing the received vector $\mathbf{y}_{S,R_g}[i]$ with the equalization matrix $\mathbf{W}_{MMSE}$, which is given by

$$\begin{aligned} \tilde{\mathbf{x}}[i] &= \mathbf{W}_{MMSE} \mathbf{y}_{S,R_g}[i] \\ &= \left(\mathbf{H}^H_{S,R_g} \mathbf{H}_{S,R_g} + \frac{\sigma_n^2}{\sigma_x^2} \mathbf{I} \right)^{-1} \mathbf{H}^H_{S,R_g} \mathbf{y}_{S,R_g}[i]. \end{aligned} \quad (6)$$

where $\sigma_n^2 = N_0$ is the power spectrum density of the AWGN and $\sigma_x^2 = E_S$ is the power of the signal. Alternative suboptimal detection techniques could also be considered in future work [38], [39], [40], [41], [42], [43], [79], [45], [**?**], [46], [47], [48], [49], [54], [55], [56].

By performing XOR network coding, only the XOR outputs (resulting M_S packets) are stored with the information: "the bit sent by S_1 is equal (or not) to the corresponding bit sent by S_2". Therefore, we apply the bitwise XOR:

$$\mathbf{z}_{[i]} = \hat{\mathbf{x}}_\mathbf{1}[i] \oplus \hat{\mathbf{x}}_\mathbf{2}[i] \quad (7)$$

and store the resulting data in the cloud buffer. Therefore, an advantage of applying XOR network coding is that we have to store only M_S packets in the cloud buffer, instead of $2M_S$.

Moreover, if the relay selection algorithm decides to operate in the BC mode, the signal sent by the relays selected for transmission R_f (R_{f_1} and R_{f_2}) and received at S_1 and S_2 is structured in an $M_S \times 1$ vector given by

$$\mathbf{y}_{R_f,S_{1(2)}}[i] = \sqrt{\frac{E_{R_f}}{2M_S}} \mathbf{H}^{v,v'}_{R_f,S_{1(2)}} \mathbf{z}[i] + \mathbf{n}_{S_{1(2)}}[i], \quad (8)$$

where $\mathbf{z}[i]$ is a $M_S \times 1$ vector with M_S symbols, $v \in \{1, 2, ..., V\}$, $v' \in \{1, 2, ..., V\}$, $\mathbf{H}^{v,v'}_{R_f,S_{1(2)}} = \mathbf{H}^{v}_{R_{f_1},S_{1(2)}} + \mathbf{H}^{v'}_{R_{f_2},S_{1(2)}}$ represents the $M_S \times M_S$ matrix of $R_{f_1}S_{1(2)}$ and $R_{f_2}S_{1(2)}$ links, and $\mathbf{n}_{S_{1(2)}}[i]$ is the AWGN at S_1 or S_2. Note that $\mathbf{H}^{v,v'}_{R_f,S_{1(2)}}$ is selected among V^2 submatrices of dimension $M_S \times M_S$ contained in $\mathbf{H}_{R_f,S_{1(2)}}$ as given by

$$\mathbf{H}_{R_f,S_{1(2)}} = [\mathbf{H}^{1,1}_{R_f,S_{1(2)}}; ...; \mathbf{H}^{1,V}_{R_f,S_{1(2)}}; ...; \mathbf{H}^{V,1}_{R_f,S_{1(2)}}; ...; \mathbf{H}^{V,V}_{R_f,S_{1(2)}}]. \quad (9)$$

We may also adopt the ML receiver at the selected cluster, which yields

$$\tilde{\mathbf{z}}_{1(2)}[i] = \arg\min_{\mathbf{z}'[i]} \left(\left\| \mathbf{y}_{R_f,S_{1(2)}}[i] - \sqrt{\frac{E_{R_f}}{2M_S}} \mathbf{H}^{v,v'}_{R_f,S_{1(2)}} \mathbf{z}'[i] \right\|^2 \right), \quad (10)$$

where $\mathbf{z}'[i]$ is each of the possible vectors with M_S symbols. In contrast, we may adopt the MMSE receiver and the solution is given by

$$\begin{aligned} \tilde{\mathbf{z}}_{1(2)}[i] &= \mathbf{W}_{MMSE} \mathbf{y}_{R_f,S_{1(2)}}[i] \\ &= \left(\mathbf{H}^{v,v'H}_{R_f,S_{1(2)}} \mathbf{H}^{v,v'}_{R_f,S_{1(2)}} + \frac{\sigma_n^2}{\sigma_x^2} \mathbf{I} \right)^{-1} \mathbf{H}^{v,v'H}_{R_f,S_{1(2)}} \mathbf{y}_{R_f,S_{1(2)}}[i]. \end{aligned} \quad (11)$$

Therefore, at S_1 we calculate the vector of symbols sent by S_2 by performing XOR type PLNC:

$$\hat{\mathbf{x}}_\mathbf{2}[i] = \mathbf{x}_\mathbf{1}[i] \oplus \hat{\mathbf{z}}_\mathbf{1}[i]. \quad (12)$$

This is also applied at S_2 to calculate the vector of symbols sent by S_1:

$$\hat{\mathbf{x}}_\mathbf{1}[i] = \mathbf{x}_\mathbf{2}[i] \oplus \hat{\mathbf{z}}_\mathbf{2}[i]. \quad (13)$$

The estimated channel matrix $\hat{\mathbf{H}}$ is considered instead of $\mathbf{H}$ in (5) and (10), when performing the ML receiver, and in (6) and (11), when performing the MMSE receiver, by assuming imperfect CSI. Note that $\hat{\mathbf{H}}$ is computed as $\hat{\mathbf{H}}$=$\mathbf{H}$+$\mathbf{H}_e$, where the variance of the mutually independent zero mean complex Gaussian $\mathbf{H}_e$ coefficients is given by $\sigma_e^2 = \beta E^{-\alpha}$ ($0 \leq \alpha \leq 1$ and $\beta \geq 0$) [33], in which $E = E_S$, in the MA phase, and $E = \frac{E_S}{2}$, in the BC phase. Channel and parameter estimation [67], [68], [69], [70], [71], [72], [74], [75], [76], [77], [78], [79], [80] and resource allocation techniques [81] could be considered in future work in order to develop algorithms for this particular setting.

III. Proposed MWC-Best-User-Link Protocol and Relay Selection Algorithms

The system presented in Fig. 1 is equipped with the novel MWC-Best-User-Link protocol, which in each time slot may operate in two possible modes: MA or BC. The relay selection algorithm needs to compute the metrics related to KNU different $2M_S \times 2M_S$ submatrices related to the uplink channels and $2KN'V^2$ different $M_S \times M_S$ submatrices related to the downlink channels, where $N' = N + C_2^N$, to select the best cluster, the best relay(s) and the mode of operation (MA or BC), in each time slot. Note that when a selected cluster formed by two source nodes is communicating with each other, the other clusters remain silent. Moreover, the relay selection algorithm may operate with two criteria: 1) using the extended MMD [16], [17] criterion; or 2) using the CNB criterion. In the first approach, if the MMD-based relay selection algorithm decides to operate in the MA mode, it chooses the relay R_g and the associated channel matrix $\mathbf{H}^{MMD}_{S,R_g}$ with the largest minimum distance as given by

$$\mathbf{H}^{MMD}_{S,R_g} = \arg\max_{\mathbf{H}_{S,R_i}} \mathcal{B}^{MA}_{min}, \quad (14)$$

where $\mathcal{B}^{MA}_{min}$ is the smallest value of the distances $\mathcal{B}^{MA} = \frac{E_S}{M_S} \left\| \mathbf{H}^u_{S,R_i}(\mathbf{x}_l - \mathbf{x}_n) \right\|^2$, $u \in \{1, \dots U\}$, $i \in \{1, \dots, N\}$, $\mathbf{x}_l$ and $\mathbf{x}_n$ represent each possible vector formed by $2M_S$ symbols and $l \neq n$. The metric $\mathcal{B}^{MA}$ is calculated for each of the $C_2^{N_s^{2M_s}}$ (combination of $N_s^{2M_S}$ in 2) possibilities, for each sub-matrix $\mathbf{H}^u_{S,R_i}$. Moreover, if the MMD-based relay selection algorithm decides to operate in the BC mode, it chooses the

relays R_f (R_{f1} and R_{f2}) and the associated channel sub-matrix $\mathbf{H}_{R_f,S}^{v,v'^{MMD}}$ with the largest minimum distance as given by

$$\mathbf{H}_{R_f,S}^{v,v'^{MMD}} = \arg \max_{\mathbf{H}_{R_{ij},S}^{v,v'}} \mathcal{B}_{min}^{BC}, \quad (15)$$

where $\mathcal{B}_{min}^{BC}$ is the smallest value of the distances $\mathcal{B}^{BC} = \frac{E_S}{2M_S} \left\| \mathbf{H}_{R_{ij},S}^{v,v'}(\mathbf{x}_l - \mathbf{x}_n) \right\|^2$, i and $j \in \{1,\ldots,N\}$, v and $v' \in \{1,\ldots,V\}$, $\mathbf{x}_l$ and $\mathbf{x}_n$ represent each possible vector formed by M_S symbols and $l \neq n$. The metric $\mathcal{B}^{BC}$ is calculated for each of the $C_2^{N_s^{M_S}}$ possibilities, for each sub-matrix $\mathbf{H}_{R_{ij},S}^{v,v'}$. In Appendix A, we develop a proof that shows that the MMD-based relay selection algorithm minimizes the PEP and also the error in the ML receiver, in the proposed MWC-Best-User-Link protocol.

In the second approach, if the CNB-based relay selection algorithm decides to operate in the MA mode, it chooses the relay R_g and the associated channel matrix $\mathbf{H}_{S,R_g}^{CNB}$ as given by

$$\mathbf{H}_{S,R_g}^{CNB} = \arg \max_{\mathbf{H}_{S,R_i}} \mathcal{C}_{min}^{MA}, \quad (16)$$

where $\mathcal{C}_{min}^{MA} = \min \left|\det(\mathbf{H}_{S,R_i}^{u})\right|$, $u \in \{1,\ldots U\}$ and $i \in \{1,\ldots,N\}$. Therefore, in the MA mode, the metric $\left|\det(\mathbf{H}_{S,R_i}^{u})\right|$ is calculated for each sub-matrix $\mathbf{H}_{S,R_i}^{u}$ and $\mathcal{C}_{min}^{MA}$ is the smallest of these values. Thus, the selected matrix $\mathbf{H}_{S,R_g}^{CNB}$ has the largest $\mathcal{C}_{min}^{MA}$ value. Moreover, if the CNB-based relay selection algorithm decides to operate in the BC mode, it chooses the relays R_f and the associated channel sub-matrix $\mathbf{H}_{R_f,S}^{v,v'^{CNB}}$ as given by

$$\mathbf{H}_{R_f,S}^{v,v'^{CNB}} = \arg \max_{\mathbf{H}_{R_{ij},S}^{v,v'}} \mathcal{C}^{BC}, \quad (17)$$

where $\mathcal{C}^{BC} = \left|\det(\mathbf{H}_{R_{ij},S}^{v,v'})\right|$. Therefore, in the BC mode, the metric $\mathcal{C}^{BC}$ is calculated for each sub-matrix $\mathbf{H}_{R_{ij},S}^{v,v'}$. Thus, the selected sub-matrix $\mathbf{H}_{R_f,S}^{v,v'^{CNB}}$ has the largest $\mathcal{C}^{BC}$ value. Note that the reason for using multiples of $2M_S$ antennas at the relays is because this relay selection criterion depends on the channel matrices $\mathbf{H}_{S,R_i}$ and $\mathbf{H}_{R_{ij},S}$ to be square or to be formed by multiple square sub-matrices. In Appendix B, we develop a proof that shows that the CNB-based relay selection algorithm maximizes the sum-rate in the MWC-Best-User-Link protocol and in Appendix C we show that this algorithm minimizes the effects of the effective noise in the MMSE receiver. Table I shows the pseudo-code of the relay selection algorithms of MWC-Best-User-Link and the following subsections explain how this protocol works.

A. Relay selection metric for MA and BC modes

For each cluster S (formed by S_1 and S_2), in the first step, we calculate the metric $\mathcal{A}_{SR_i}^{u}$ related to the SR links of each square sub-matrix $\mathbf{H}_{S,R_i}^{u}$ associated with R_i, in the MA mode:

$$\mathcal{A}_{SR_i}^{u} = \begin{cases} \mathcal{C}^{MA} = \left|\det\left(\mathbf{H}_{S,R_i}^{u}\right)\right|, & \text{for CNB,} \\ \mathcal{B}_{min}^{MA}, & \text{for MMD,} \end{cases}$$

TABLE I
MULTI-WAY CLOUD-DRIVEN BEST-USER-LINK: PSEUDO-CODE OF THE RELAY SELECTION ALGORITHMS

1: Calculate $\mathcal{A}_{SR_i}^{u}$ of each sub-matrix $\mathbf{H}_{S,R_i}^{u}$ of R_i, for MA mode:
$\mathcal{A}_{SR_i}^{u} = \begin{cases} \mathcal{C}^{MA} = \left|\det\left(\mathbf{H}_{S,R_i}^{u}\right)\right|, & \text{for CNB,} \\ \mathcal{B}_{min}^{MA}, & \text{for MMD,} \end{cases}$
2: Compute the ordering on $\mathcal{A}_{SR_i}^{u}$ and find the smallest metric:
$\mathcal{A}_{SR_i} = \min(\mathcal{A}_{SR_i}^{u})$.
3: Compute the ordering on $\mathcal{A}_{SR_i}$ and find the largest metric for each cluster:
$\mathcal{A}_{k_{\max SR}} = \max(\mathcal{A}_{SR_i})$.
4: Compute the ordering and find the largest metric:
$\mathcal{A}_{\max SR} = \max(\mathcal{A}_{k_{\max SR}})$.
5: Calculate $\mathcal{A}_{R_{ij}S_1}^{v,v'}$ of each sub-matrix $\mathbf{H}_{R_{ij},S_1}^{v,v'}$ of R_i and R_j, for BC mode:
$\mathcal{A}_{R_{ij}S_1}^{v,v'} = \begin{cases} \mathcal{C}^{BC} = \left|\det\left(\mathbf{H}_{R_{ij},s_1}^{v,v'}\right)\right|, & \text{for CNB,} \\ \mathcal{B}_{min}^{BC}, & \text{for MMD,} \end{cases}$
6: Calculate the metric $\mathcal{A}_{R_{ij}S_2}^{v,v'}$ of each sub-matrix $\mathbf{H}_{R_{ij},s_2}^{v,v'}$.
7: Compare the metrics $\mathcal{A}_{R_{ij}S_1}^{v,v'}$ and $\mathcal{A}_{R_{ij}S_2}^{v,v'}$ and store the smallest one:
$\mathcal{A}_{R_{ij}S}^{v,v'} = \min(\mathcal{A}_{R_{ij}S_1}^{v,v'}, \mathcal{A}_{R_{ij}S_2}^{v,v'})$.
8: Compute the ordering and find the largest metric:
$\mathcal{A}_{R_{ij}S} = \max(\mathcal{A}_{R_{ij}S}^{v,v'})$
9: Compute the ordering and find the largest metric, for each cluster:
$\mathcal{A}_{k_{\max RS}} = \max(\mathcal{A}_{R_{ij}S})$.
10: Compute the ordering and find the largest metric:
$\mathcal{A}_{\max RS} = \max(\mathcal{A}_{k_{\max RS}})$.
11: Select the transmission mode
$\begin{cases} \text{if } \frac{N_{packets}}{M_S} > LoL, \text{ then} & \text{" BC mode" and select the cluster,} \\ & \text{whose buffer is fullest.} \\ \text{elseif } \frac{\mathcal{A}_{\max SR}}{\mathcal{A}_{\max RS}} \geq G, \text{ then} & \text{" MA mode",} \\ \text{otherwise,} & \text{" BC mode".} \end{cases}$

where $u \in \{1,...,U\}$ and $i \in \{1,...,N\}$. In the second step, we compute the ordering on $\mathcal{A}_{SR_i}^{u}$ and find the smallest metric:

$$\mathcal{A}_{SR_i} = \min(\mathcal{A}_{SR_i}^{u}), \quad (18)$$

In the third step, we compute the ordering on $\mathcal{A}_{SR_i}$ and find the largest metric:

$$\mathcal{A}_{k_{\max SR}} = \max(\mathcal{A}_{SR_i}), \quad (19)$$

where $k \in \{1,...,K\}$. After finding $\mathcal{A}_{k_{\max SR}}$ for each cluster, we compute the ordering and find the largest metric:

$$\mathcal{A}_{\max SR} = \max(\mathcal{A}_{k_{\max SR}}). \quad (20)$$

Therefore, we choose the cluster and the relay R_i that fulfil (20) to receive M_S packets from the selected cluster. For each cluster, in the fourth step, we calculate the metrics $\mathcal{A}_{R_{ij}S_1}$ related to the RS_1 links of each sub-matrix $\mathbf{H}_{R_{ij},S_1}^{v,v'}$ associated with each pair R_i and R_j, for BC mode:

$$\mathcal{A}_{R_{ij}S_1}^{v,v'} = \begin{cases} \mathcal{C}^{BC} = \left|\det\left(\mathbf{H}_{R_{ij},S_1}^{v,v'}\right)\right|, & \text{for CNB,} \\ \mathcal{B}_{min}^{BC}, & \text{for MMD,} \end{cases}$$

where $\mathbf{H}_{R_{ij},S_1}^{v,v'} = \mathbf{H}_{R_i,S_1}^{v} + \mathbf{H}_{R_j,S_1}^{v'}$, v and $v' \in \{1,...,V\}$, i and $j \in \{1,...,N\}$.

In the fifth step, this reasoning is also applied to calculate the metric $\mathcal{A}^{v,v'}_{R_{ij}S_2}$. In the sixth step, we compare the metrics $\mathcal{A}^{v,v'}_{R_{ij}S_1}$ and $\mathcal{A}^{v,v'}_{R_{ij}S_2}$ and store the smallest one:

$$\mathcal{A}^{v,v'}_{R_{ij}S} = \min(\mathcal{A}^{v,v'}_{R_{ij}S_1}, \mathcal{A}^{v,v'}_{R_{ij}S_2}). \tag{21}$$

After finding $\mathcal{A}^{v,v'}_{R_{ij}S}$ for each pair of sub-matrices $\mathbf{H}^{v,v'}_{R_{ij},S_1}$ e $\mathbf{H}^{v,v'}_{R_{ij},S_2}$, we compute the ordering and find the largest metric:

$$\mathcal{A}_{R_{ij}S} = \max(\mathcal{A}^{v,v'}_{R_{ij}S}). \tag{22}$$

In the seventh step, after finding $\mathcal{A}_{R_{ij}S}$ for each pair of relays, we compute the ordering and find the largest metric:

$$\mathcal{A}_{k_{\max RS}} = \max(\mathcal{A}_{R_{ij}S}), \tag{23}$$

where $k \in \{1, ..., K\}$. After finding $\mathcal{A}_{k_{\max RS}}$ for each cluster, we compute the ordering and find the largest metric:

$$\mathcal{A}_{\max RS} = \max(\mathcal{A}_{k_{\max RS}}). \tag{24}$$

Therefore, we select the cluster and the relays R_i and R_j that fulfil (24) to send simultaneously M_S packets stored in the associated cloud buffer to the selected cluster. The estimated channel matrix $\hat{\mathbf{H}}$ is considered, instead of $\mathbf{H}$, if we consider imperfect CSI. Additionally, a designer might consider precoding and beamforming techniques [57], [58], [59], [60], [61], [62], [63], [64], [65], [66], [72], [73], [53], [50], [51], [52] to help mitigate interference rather thanopen loop transmission.

B. Choice of the transmission mode

After calculating the metrics related to the SR and RS links and finding $\mathcal{A}_{\max SR}$ and $\mathcal{A}_{\max RS}$, these metrics are compared and we select the transmission mode:

$$\begin{cases} \text{if } \frac{N_{packets}}{M_S} > LoL, \text{ then} & \text{" BC mode" and select the cluster} \\ & \text{whose buffer is fullest.} \\ \text{elseif } \frac{\mathcal{A}_{\max SR}}{\mathcal{A}_{\max RS}} \geq G, \text{ then} & \text{" MA mode",} \\ \text{otherwise,} & \text{" BC mode",} \end{cases}$$

where $G = \frac{E[\mathcal{A}_{\max SR}]}{E[\mathcal{A}_{\max RS}]}$, $N_{packets}$ is the total number of packets stored in the cloud buffers, LoL is a parameter that when reduced increases the probability of the protocol to operate in BC mode and, consequently, to achieve a reduced average delay (low latency).

IV. Analysis

In this section, the PEP of the proposed MWC-Best-User-Link protocol is analysed and expressions for the sum-rate and average delay of MWC-Best-User-Link are derived. Moreover, the cost of MWC-Best-User-Link and existing protocols is also examined.

A. Pairwise Error Probability

The PEP assumes an error event when $\mathbf{x}_n$ is sent and the detector calculates an incorrect $\mathbf{x}_l$ (where $l \neq n$), based on the received symbol [15], [16], [17]. Considering $\mathcal{D}' = \|\mathbf{H}(\mathbf{x}_n - \mathbf{x}_l)\|^2$, in the MA mode, and $\mathcal{D}' = \frac{1}{2}\|\mathbf{H}(\mathbf{x}_n - \mathbf{x}_l)\|^2$, in BC mode, the PEP is given by

$$\mathbf{P}(\mathbf{x}_n \to \mathbf{x}_l|\mathbf{H}) = Q\left(\sqrt{\frac{E_s}{2N_0M_S}\mathcal{D}'}\right). \tag{25}$$

We may consider that the worst value of the PEP occurs for the smallest value of $\mathcal{D}'$ and then the PEP worst case ($\mathcal{D}'_{\min}$) is given by

$$\mathbf{P}(\mathbf{x}_n \to \mathbf{x}_l|\mathbf{H}) = Q\left(\sqrt{\frac{E_S}{2N_0M_S}\mathcal{D}'_{\min}}\right). \tag{26}$$

Assuming that the probability of having no error in the two phases of the system is approximately given by the square of $(1 - \mathbf{P}(\mathbf{x}_n \to \mathbf{x}_l|\mathbf{H}))$, an expression for calculating the worst case of the PEP for cooperative transmissions (CT), in each time slot is given by

$$\begin{aligned} \mathbf{P}^{CT}(\mathbf{x}_n \to \mathbf{x}_l|\mathbf{H}) &= 1 - (1 - \mathbf{P}(\mathbf{x}_n \to \mathbf{x}_l|\mathbf{H}))^2 \\ &= 1 - \left(1 - Q\left(\sqrt{\frac{E_S}{2N_0M_S}\mathcal{D}'_{\min}}\right)\right)^2. \end{aligned} \tag{27}$$

Note that this expression may be used for calculating the worst case of the PEP, for both symmetric and asymmetric channels.

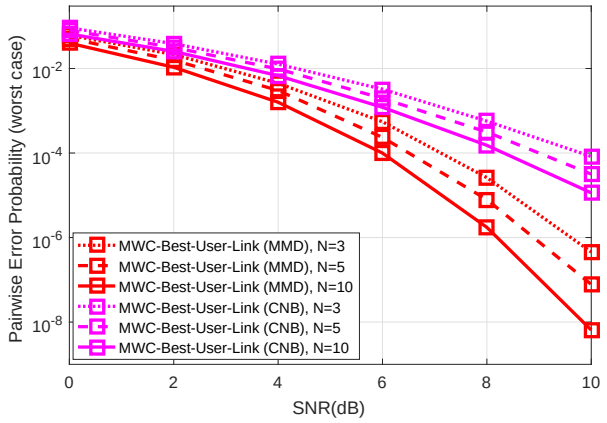

Fig. 3. Theoretical PEP performance versus SNR.

Fig. 3 illustrates the theoretical PEP performance (computed by the algorithm based on the selected channel matrix $\mathbf{H}$, in each time slot) of MWC-Best-User-Link (MMD) and MWC-Best-User-Link (CNB) protocols, for $M_S = 2$, $M_{R_{rx}} = 4$ ($U = 1$), $M_{R_{tx}} = 2$ ($V = 1$), $K = 3$, $N = 3$, 5 and 10, $LoL > KL$, perfect CSI, BPSK and unit power symmetric channels. By maximizing the metric $\mathcal{D}'_{\min}$, the extended MMD criterion minimizes the worst case of the PEP in the MWC-Best-User-Link protocol. Otherwise, while not taking into account $\mathcal{D}'_{\min}$, CNB maximizes the sum-rate in the MWC-Best-User-Link protocol and has low computational cost.

B. Sum-Rate

The system capacity upper bounds the sum-rate of a given system [14]. In MWC-Best-User-Link, as the relay selected for reception R_g may be different from the relay selected for transmission R_f, its capacity is given by [37]:

$$C_{DF} = \frac{1}{2}\min\{I_{DF}^{SR_g}, I_{DF}^{R_fS}\}, \quad (28)$$

where the terms in (28) are the maximum rate at which R_g can reliably decode the data sent by the selected cluster S_1 and S_2 and at which this selected cluster can reliably decode the estimated data sent by R_f, respectively. In [17], the relationship between mutual information and entropy is established for a given channel matrix $\mathbf{H}_{S,R_g}$ and the maximum mutual information is given by

$$I_{DF}^{SR_g} = \log_2 \det\left(\mathbf{H}_{S,R_g}(\mathbf{Q}_{S,R_g}/N_0)\mathbf{H}_{S,R_g}^H + \mathbf{I}\right), \quad (29)$$

where $\mathbf{Q}_{S,R_g} = E[\mathbf{x}(\mathbf{x})^H] = \mathbf{I}\,\frac{E_S}{M_S}$, and the vectors $\mathbf{x}$ are structured by independent and identically distributed (i.i.d.) transmitted symbols. This also can be applied to $I_{DF}^{R_fS}$:

$$I_{DF}^{R_fS} = \log_2 \det\left(\mathbf{H}_{R_f,S}(\mathbf{Q}_{R_f,S}/N_0)\mathbf{H}_{R_f,S}^H + \mathbf{I}\right), \quad (30)$$

where $\mathbf{Q}_{R_f,S} = \mathbf{I}\,\frac{E_S}{2M_S}$. However, instead of considering the minimum of the terms in (28), to calculate the sum-rate of the proposed protocol, we employ an approximated expression given by the average of the values found in each time slot. Therefore, in the case of a time slot i selected for MA mode, the sum-rate is given by

$$\mathcal{R}_i^{SR} = \frac{1}{2}\ \log_2 \det\left(\mathbf{H}_{S,R_g}(\mathbf{Q}_{S,R_g}/N_0)\mathbf{H}_{S,R_g}^H + \mathbf{I}\right). \quad (31)$$

Furthermore, in the case of a time slot i selected for BC mode, the sum-rate is given by

$$\mathcal{R}_i^{RS_{1(2)}} = \frac{1}{2}\ \log_2 \det\left(\mathbf{H}_{R_f,S_{1(2)}}(\mathbf{Q}_{R_f,S_{1(2)}}/N_0)\mathbf{H}_{R_f,S_{1(2)}}^H + \mathbf{I}\right)$$

Therefore, by summing the sum-rate values found in each time slot and dividing this result by the total number of time slots, we have that the average sum-rate ($\mathcal{R}$) of the MWC-Best-User-Link scheme can be approximated by

$$\mathcal{R} \approx \frac{\sum_{i=1}^{n_{SR}} \mathcal{R}_i^{SR} + \sum_{i=1}^{n_{RS}} (\mathcal{R}_i^{RS_1} + \mathcal{R}_i^{RS_2})}{n_{SR} + n_{RS}}, \quad (33)$$

where n_{SR} and n_{RS} are the number of time slots selected for SR and RS transmissions, respectively.

C. Computational Cost

The number of operations of the relay selection algorithm of the proposed MWC-Best-User-Link is related to the complexity of the CNB or MMD[15], [16], [17] criterion. Table II shows the complexity of the relay selection algorithm in the proposed MWC-Best-User-Link (using the CNB criterion), and the existing MW-Max-Link [15], TW-Max-Link [18] and TW-Max-Min [11], here adapted for multiple-antenna systems (using the MMD criterion), for K clusters, N relays, M_S antennas at the users, $M_{R_{rx}} = 2UM_S$ antennas at the relays and $M_{R_{tx}} = M_S$ (selected out of VM_S), considering

TABLE II
COMPUTATIONAL COST

Protocols	additions	multiplications
MWC-Best-User-Link	$2KN'V^2\mathcal{X} + KUN\mathcal{Y}$	$2KN'V^2\mathcal{Z} + KUN\mathcal{J}$
MW-Max-Link [15]	$KNM_S(\mathcal{U}^{total} - 3)$	$KNM_S(\mathcal{U}^{total})$
TW-Max-Link [18]	$NM_S(\mathcal{U}^{total} - 3)$	$NM_S(\mathcal{U}^{total})$
TW-Max-Min [11]	$\frac{NM_S}{2}(\mathcal{U}^{total} - 3)$	$\frac{NM_S}{2}(\mathcal{U}^{total})$

$N' = N + C_2^N$, $\mathcal{X} = 0$, if $M_S = 1$, $\mathcal{X} = 1$, if $M_S = 2$, and $\mathcal{X} = 2M_S - 1$, if $M_S \geq 3$, $\mathcal{Y} = 1$, if $M_S = 1$, $\mathcal{Y} = 4M_S - 1$, if $M_S \geq 2$, $\mathcal{Z} = 0$, if $M_S = 1$, $\mathcal{Z} = 2$, if $M_S = 2$, and $\mathcal{Z} = 2(M_S^2 - M_S)$, if $M_S \geq 3$, $\mathcal{J} = 2$, if $M_S = 1$, $\mathcal{J} = 4M_S^2 - 2M_S$, if $M_S \geq 2$, and the number of calculations of the MMD metric for each relay is given by

$$\mathcal{U}^{total} = \sum_{i=1}^{2M_S} 2^{i-1}W^i C_i^{2M_S} + 2\sum_{i=1}^{M_S} 2^{i-1}W^i C_i^{M_S}, \quad (34)$$

where W (quantity of distances between the constellation symbols) equals 1, for BPSK, and equals 3, for QPSK. Fig.

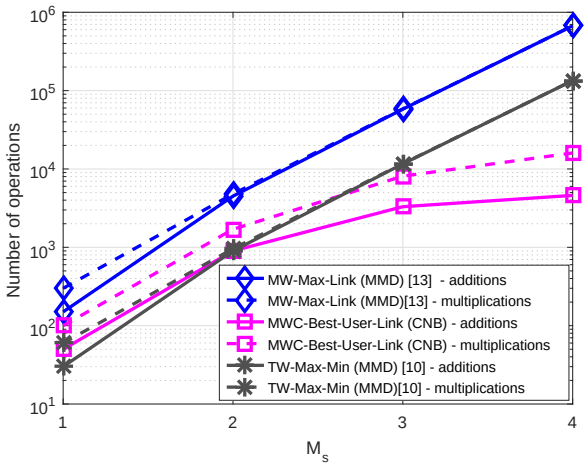

Fig. 4. Computational cost.

4 shows the complexity of the relay selection algorithm in MWC-Best-User-Link (CNB), MW-Max-Link (MMD) and TW-Max-Min (MMD), for $M_{R_{rx}} = 2M_S$ ($U = 1$) and $M_{R_{tx}} = M_S$ ($V = 1$), $K = 5$, $N = 10$ and BPSK. From this result, we notice that the complexity of the relay selection algorithm in MWC-Best-User-Link (CNB) is smaller than the complexity of the relay selection algorithm in MW-Max-Link (MMD). If we increase the number of antennas to $M_S = 3$ (or more) the complexity of the MMD criterion is considerably greater than that of CNB.

D. Average Delay

In [12], a framework based on Discrete Time Markov Chains (DTMC) is proposed to analyze the traditional Max-Link algorithm, that considers single-antenna systems. This framework has been used in many subsequent works to analyze other buffer-aided relay selection protocols whose buffer is finite [34]. Moreover, in [34], this framework is used to

analyze the average delay of an approach based on the Max-Link algorithm. In the following, we use this framework to analyze the average delay of the existing MW-Max-Link [15] and the proposed MWC-Best-User-Link protocols for multiple-antenna systems.

Similarly to Max-Link [12], MW-Max-Link [15] was originally considered for applications without critical delay constraints. In this work, by considering the importance of a short average delay in most modern applications, an expression for the average delay of the proposed MWC-Best-User-Link protocol is presented. The average delay is calculated by considering the time a packet needs to reach the destination once it has left the source (no delay is measured when the packet resides at the source [34]). So, the delay is the number of time slots the packet stays in the buffer of the relay [34]. In MW-Max-Link, each relay is equiped with a set of K buffers (each cluster has a particular buffer in the relays). For i.i.d. channels, the average delay is the same on all relays. Hence, it is sufficient to analyze the average delay on a single relay [34]. By Little's law, the average packet delay at relay's buffer R_j, denoted by $E[d_j]$ is given by

$$E[d_j] = \frac{E[L_j]}{E[T_j]}, \tag{35}$$

where $E[L_j]$ and $E[T_j]$ are the average queue length and average throughput, respectively [34]. The derivation for the average delay at the high SNR regime is given in [35]. As the selection of a relay's buffer is equiprobable, the average throughput at any relay's buffer R_j is $\frac{\rho}{NK}$, where ρ is the average data rate. Since we have half-duplex links $\rho = 1/2$ and therefore $E[T_j] = \frac{1}{2NK}$. Then, assuming an ideal balance between the operating modes (MA and BC), it can be shown that the average queue length at any relay is $E[L_j] = \frac{L}{2}$, where $L = \frac{J}{M_S}$. Thus, by Little's law, the average delay in the MW-Max-Link protocol is given by

$$E[d_j]^{BA} = E[d]^{BA} = NKL. \tag{36}$$

However, due to a possible unbalance between the operating modes, $E[L_j]$ may be smaller or larger than $\frac{L}{2}$, $(E[L_j] < L)$, and, consequently, $E[d_j]^{BA} < 2NKL$. So, as either the number of relays, the number of clusters or the buffer size increases, the average delay of MW-Max-Link increases. In contrast, in the Cloud-Driven MWC-Best-User-Link protocol, there is a unique set of K buffers that resides in the cloud. Consequently, as the number of relays increases, the average delay remains the same. Thus, by considering an ideal balance between the operating modes, the average delay in the proposed MWC-Best-User-Link is given by

$$E[d]^{CD} = KL. \tag{37}$$

However, with a possible unbalance between the operating modes, the same reasoning is applied and, consequently, $E[d_j]^{CD} < 2KL$. Nevertheless, the average delay can be further reduced by forcing the protocol to operate in BC mode and to select the cluster whose buffer is fullest, when the number of sets of M_S packets in the cloud buffers is greater than the low latency parameter LoL. By using LoL, considering an ideal balance between the operation modes, we have:

$$E[d]^{CD} = \begin{cases} 1, \text{ if } LoL = 0, \\ KL, \text{ if } LoL > KL. \end{cases} \tag{38}$$

or

$$E[d]^{CD} \approx LoL, \text{ if } 0 < LoL \leq KL, \tag{39}$$

and by considering a possible unbalance between the operating modes, the same reasoning applies.

V. Simulation Results

We assess via simulations the proposed MWC-Best-User-Link and the existing MW-Max-Link [15], using the CNB-based and the extended MMD-based relay selection algorithms. We employ BPSK signals and note that other constellations as QPSK and 16-QAM were not included but can be examined elsewhere. The performance of MWC-Best-User-Link and MW-Max-Link protocols was assessed for a set of L values. Then, we found that $L = \frac{J}{M_S} = 3$ sets of M_S packets is sufficient to ensure a good performance. We consider perfect and imperfect CSI, symmetric unit power channels ($\sigma^2_{S,R} = \sigma^2_{R,S} = 1$) and also asymmetric channels. We consider heterogeneous [31] and homogeneous path-loss. As an example, in the simulated configuration with heterogeneous distances and path-loss, the distance between each source S_k (S_{1_k} or S_{2_k}) and each relay R_i is given by $d_{S_k,R_i} = \frac{d_{S_{k=1},R_i}}{1-0.1(k-1)}$ and the path-loss between each source S_k (S_{1_k} or S_{2_k}) and each relay R_i is given by $\xi_{S_k,R_i} = \xi_{S_{k=1},R_i} \times (1 + 0.25(k-1))$. In contrast, by considering homogeneous distances and path-loss, the source and relay nodes are distributed with different locations, but the relays have approximately equal distances and path-loss to the sources. Thus, the system model is simplified and given by $\mathbf{H}_{S_k,R_i} = \mathbf{G}_{S_k,R_i}$. Moreover, we consider time-uncorrelated and time-correlated channels. As an example, in the simulated configuration with time-correlated channels, the channel matrix in each time slot is given by $\mathbf{H}_{t+1} = \rho\mathbf{H}_t + \sqrt{1-\rho^2}\mathbf{H}_p$, where $\mathbf{H}_t$ is the channel matrix in the previous time-slot, $-1 \leq \rho \leq 1$ and $\mathbf{H}_p$ is also a channel matrix formed by mutually independent zero mean complex Gaussian random coefficients ($\rho = 0$, for time-uncorrelated channels). The signal-to-noise ratio (SNR) given by E/N_0 ranges from 0 to 10 dB, where E is the energy transmitted from each source or the relay(s) and we consider $N_0 = 1$. The transmission protocols were simulated for $10000M_S$ packets, each with $T = 100$ symbols. We assumed perfect signaling between the cloud and the relays, but imperfect signaling can be considered in future works.

A. PEP and Sum-Rate performances

In this section we present the theoretical PEP (computed by the algorithm based on the selected channel matrix $\mathbf{H}$, in each time slot) and the sum-rate performance obtained by simulation of the proposed MWC-Best-User-Link (using CNB and MMD) and the existing MW-Max-Link [15], TW-Max-Link [18] and TW-Max-Min [11] (using MMD).

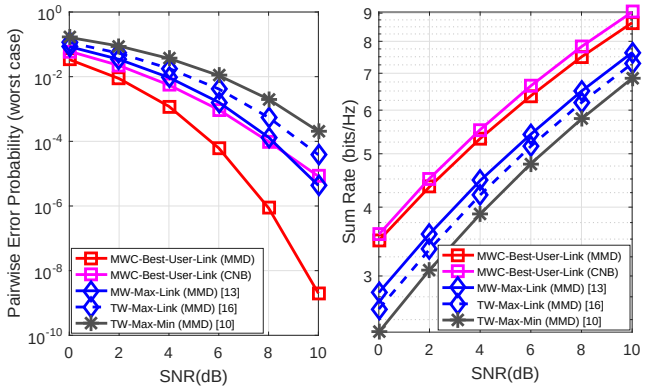

Fig. 5. PEP and Sum-Rate performances versus SNR.

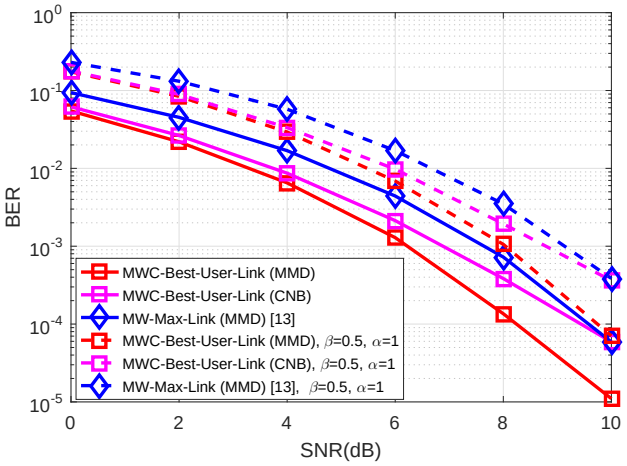

Fig. 6. BER performance versus SNR.

Fig. 5 illustrates the Sum-Rate and the theoretical PEP performances, for homogeneus path-loss, Gaussian distributed signals and BPSK, respectively, of MWC-Best-User-Link (MMD), MWC-Best-User-Link (CNB), MW-Max-Link (MMD)[15], TW-Max-Link (MMD)[18] and TW-Max-Min (MMD)[11] protocols, for $M_S = 2$, $M_{R_{rx}} = 4$ ($U = 1$), $M_{R_{tx}} = 2$ ($V = 1$), $K = 5$, $N = 10$, $LoL > KL$, perfect CSI and unit power symmetric channels. The PEP performance of MWC-Best-User-Link (MMD) is considerably better than that of MWC-Best-User-Link (CNB), as MMD maximizes the metric $\mathcal{D}'_{\min}$, and the PEP performance of MWC-Best-User-Link (CNB) is close to the performance of MW-Max-Link. Nevertheless, the sum-rate performances of the MWC-Best-User-Link (MMD) and MWC-Best-User-Link (CNB) are considerably better than those of the other protocols for all the range of SNR values simulated. Moreover, the sum-rate performance of MWC-Best-User-Link (CNB) is superior to that of MWC-Best-User-Link (MMD), as CNB maximizes the sum-rate.

B. BER and Average Delay performances with the ML receiver

In this section we present the BER and average delay performances of the proposed MWC-Best-User-Link (using the CNB-based and the extended MMD-based relay selection algorithms) and MW-Max-Link [15], using MMD, with the ML receiver, for homogeneous path-loss and time-uncorrelated channels.

Fig. 6 depicts the BER performance of the MWC-Best-User-Link (MMD), MWC-Best-User-Link (CNB) and MW-Max-Link (MMD) protocols, for homogeneous path-loss, $M_S = 2$, $M_{R_{rx}} = 4$ ($U = 1$), $M_{R_{tx}} = 2$ ($V = 1$), $K = 5$, $N = 10$, BPSK, $LoL > KL$, perfect and imperfect CSI ($\beta = 0.5$ and $\alpha = 1$) and unit power symmetric channels. For both perfect and imperfect CSI (full and dashed curves, respectively), MWC-Best-User-Link (MMD) outperforms MWC-Best-User-Link (CNB), mainly for SNR values greater than 6dB, as MMD maximizes the metric $\mathcal{D}'_{\min}$. MWC-Best-User-Link (MMD) also outperforms MW-Max-Link for the range of SNR values simulated. Moreover, MWC-Best-User-Link (CNB) outperforms MW-Max-Link for SNR values less than 10dB. The results shown in Figs. 5 and 6 demonstrate the benefits of joint detection provided by the cloud-driven framework.

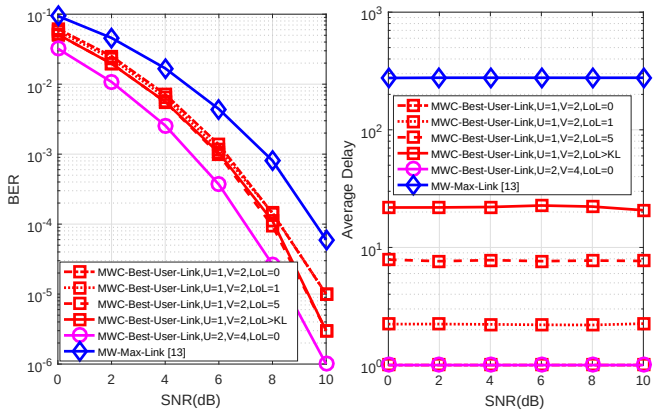

Fig. 7. BER and Average Delay performances versus SNR.

Fig. 7 illustrates the BER and the average delay performances of MWC-Best-User-Link (MMD) and MW-Max-Link (MMD) protocols, for homogeneous path-loss, BPSK, $M_S = 2$, $M_{R_{rx}} = 4$ and 8 ($U = 1$ and 2), $M_{R_{tx}} = 2$ ($V = 2$ and 4), $K = 5$, $N = 10$, $LoL = 0$, 1, 5 and $LoL > KL$, perfect CSI and unit power symmetric channels. The average delay performance of MWC-Best-User-Link is considerably better than that of MW-Max-Link, as MWC-Best-User-Link has a unique set of K cloud buffers. When we reduce the value of LoL to 0 in the MWC-Best-User-Link protocol, the average delay is reduced to 1 time slot, keeping almost the same BER performance. This result validates our analysis in Section IV. Moreover, the BER performance of MWC-Best-User-Link is considerably better than that of MW-Max-Link for $U = 1$ and $V = 2$. For higher values of U and V the BER performance of MWC-Best-User-Link is considerably improved, due to a higher diversity gain in the uplink and the antenna selection in the downlink.

Fig. 8 illustrates the BER and the average delay per-

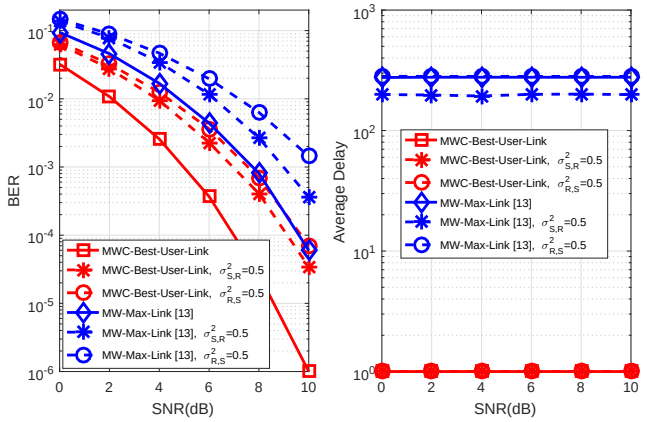

Fig. 8. BER and Average Delay performances versus SNR.

formances of MWC-Best-User-Link (MMD) and MW-Max-Link (MMD) protocols, for homogeneous path-loss, BPSK, $M_S = 2$, $M_{R_{rx}} = 8$ ($U = 2$), $M_{R_{tx}} = 2$ ($V = 4$), $K = 5$, $N = 10$, $LoL = 0$, symmetric ($\sigma^2_{S,R} = \sigma^2_{R,S} = 1$) and asymmetric channels ($\sigma^2_{S,R} = 1$ and $\sigma^2_{R,S} = 0.5$ or $\sigma^2_{S,R} = 0.5$ and $\sigma^2_{R,S} = 1$) and perfect CSI. The average delay performance of MWC-Best-User-Link is considerably better than that of MW-Max-Link. When LoL equals 0 in the MWC-Best-User-Link protocol, the average delay equals 1 time slot and the BER performance of MWC-Best-User-Link is considerably better than that of MW-Max-Link, for both symmetric and asymmetric channels. If we consider higher values of U and V, the BER performance of MWC-Best-User-Link can be further improved.

C. BER and Average Delay performances with the MMSE receiver

In this section we present the BER and average delay performances of the proposed MWC-Best-User-Link (using the CNB-based and the extended MMD-based relay selection algorithms) and MW-Max-Link [15], using CNB, with the linear MMSE receiver, for homogeneous path-loss and time-uncorrelated channels.

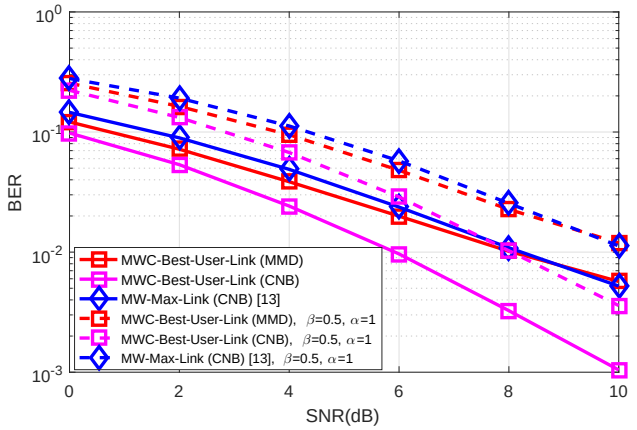

Fig. 9. BER performance versus SNR.

Fig. 9 depicts the BER performance of the MWC-Best-User-Link (MMD), MWC-Best-User-Link (CNB) and MW-Max-Link (CNB) protocols, for homogeneous path-loss, $M_S = 2$, $M_{R_{rx}} = 4$ ($U = 1$), $M_{R_{tx}} = 2$ ($V = 1$), $K = 5$, $N = 10$, BPSK, $LoL > KL$, perfect and imperfect CSI ($\beta = 0.5$ and $\alpha = 1$) and unit power symmetric channels. For both perfect and imperfect CSI (full and dashed curves, respectively), the BER performance of MWC-Best-User-Link (CNB) is considerably better than that of MWC-Best-User-Link (MMD), as CNB minimizes the error in the MMSE receiver and MMD is based on the ML principle and the PEP. Moreover, MWC-Best-User-Link (CNB) also outperforms MW-Max-Link (CNB) for all the range of SNR values simulated.

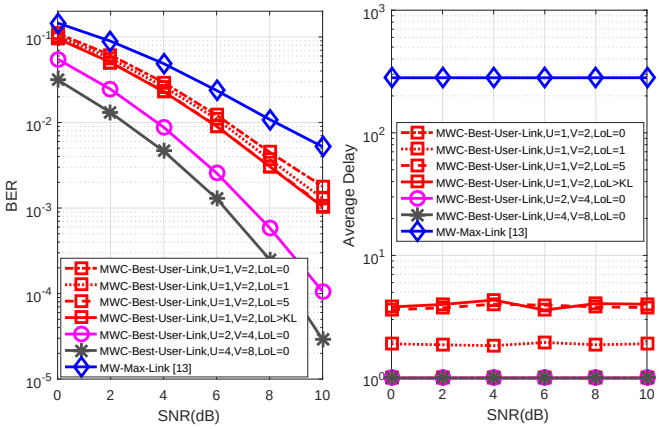

Fig. 10. BER and Average Delay performances versus SNR.

Fig. 10 illustrates the BER and the average delay performances of MWC-Best-User-Link (CNB) and MW-Max-Link (CNB), for homogeneous path-loss, BPSK, $M_S = 2$, $M_{R_{rx}} = 4$, 8 and 16 ($U = 1$, 2 and 4), $M_{R_{tx}} = 2$ ($V = 2$, 4 and 8), $K = 5$, $N = 10$, $LoL = 0$, 1, 5 and $LoL > KL$, perfect CSI and unit power symmetric channels. The average delay performance of MWC-Best-User-Link is considerably better than that of MW-Max-Link, as MWC-Best-User-Link has a unique set of K cloud buffers. When we reduce the value of LoL to 0 in the MWC-Best-User-Link protocol, the average delay is reduced to 1 time slot, keeping almost the same BER performance. Moreover, the BER performance of MWC-Best-User-Link is considerably better than that of MW-Max-Link for $U = 1$ and $V = 2$. For higher values of U and V the BER performance of MWC-Best-User-Link is considerably improved, due to a higher diversity gain in the uplink and the antenna selection in the downlink.

Fig. 11 illustrates the BER and the average delay performances of MWC-Best-User-Link (CNB) and MW-Max-Link (CNB) protocols, for homogeneous path-loss, BPSK, $M_S = 2$, $M_{R_{rx}} = 8$ ($U = 2$), $M_{R_{tx}} = 2$ ($V = 4$), $K = 5$, $N = 10$, $LoL = 0$, symmetric ($\sigma^2_{S,R} = \sigma^2_{R,S} = 1$) and asymmetric channels ($\sigma^2_{S,R} = 1$ and $\sigma^2_{R,S} = 0.5$ or $\sigma^2_{S,R} = 0.5$ and $\sigma^2_{R,S} = 1$) and perfect CSI. The average delay performance of MWC-Best-User-Link is considerably better than that of MW-Max-Link. When LoL equals 0 in the MWC-Best-User-Link protocol, the average delay equals 1 time slot and the

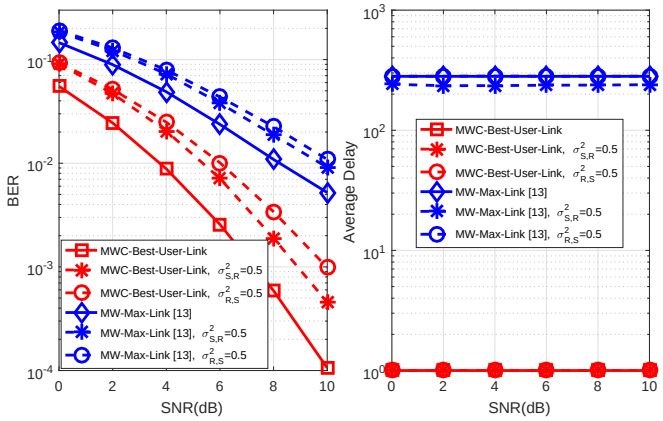

Fig. 11. BER and Average Delay performances versus SNR.

BER performance of MWC-Best-User-Link is considerably better than that of MW-Max-Link, for both symmetric and asymmetric channels. If we consider higher values of U and V, the BER performance of MWC-Best-User-Link can be further improved.

D. BER and Sum-Rate performances, for heterogeneous path-loss and time-correlated channels

In this section we present the BER and sum-rate performances of the proposed MWC-Best-User-Link and the existing MW-Max-Link [15] (using the extended MMD-based relay selection algorithm with the linear ML receiver and the CNB-based relay selection algorithm with the linear MMSE receiver), for heterogeneous path-loss and time-correlated channels.

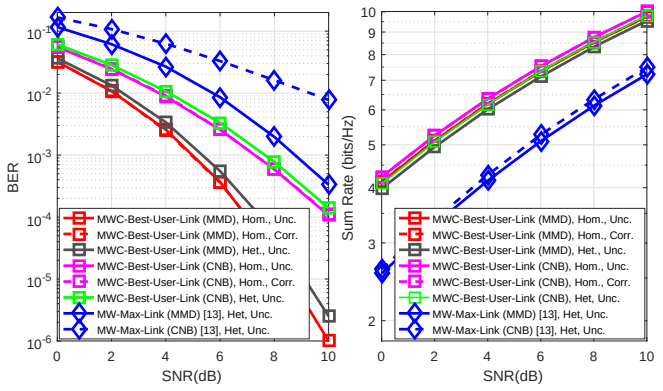

Fig. 12. BER and Sum-Rate performances versus SNR.

Fig. 12 illustrates the BER and the sum-rate performances of MWC-Best-User-Link (MMD) and MWC-Best-User-Link (CNB) protocols, considering 3 different configurations: a) homogeneous path-loss and time-uncorrelated channels, b) homogeneous path-loss and time-correlated channels ($\rho^2 = 0.9$), c) heterogeneous path-loss and time-uncorrelated channels, for BPSK, $M_S = 2$, $M_{R_{rx}} = 8$ ($U = 2$), $M_{R_{tx}} = 2$ ($V = 4$), $K = 5$, $N = 10$, $LoL = 0$ and perfect CSI. The BER and sum-rate performances of MWC-Best-User-Link are the same for time-uncorrelated or time-correlated channels, as these protocols select the best links in each time slot. Moreover, the BER and sum-rate performances of MWC-Best-User-Link considering heterogeneous path-loss are almost equal to that for homogeneous path-loss, as the links selected by the proposed protocol tends to be associated with the cluster of users which is closest to the cluster of relays. Furthermore, the BER and sum-rate performances of MWC-Best-User-Link considering heterogeneous path-loss are considerably better than those of MW-Max-Link.

VI. Conclusion

A novel framework using a cloud as a central node with buffers has been introduced and investigated as a favorable relay selection strategy for multi-way protocols. We have examined relay-selection techniques for multi-way cooperative MIMO systems that are driven by a cloud central node, where a cluster with two sources is selected to simultaneously transmit to each other aided by relays. In order to perform signal detection at the cloud and the nodes, we have presented ML and linear MMSE detectors. Simulations illustrate the excellent performance of the proposed MWC-Best-User-Link protocol, that by using the novel CNB-based or the extended MMD-based relay selection algorithm outperformed the existing MW-Max-Link scheme in terms of PEP, sum-rate, average delay and computational cost. In particular, this novel protocol has a considerably reduced average delay, keeping the high diversity gain, both for MMSE and ML detection. Moreover, MWC-Best-User-Link (MMD) has the best performance when ML detection is used, as the MMD criterion minimizes the error in the ML receiver. In contrast, MWC-Best-User-Link (CNB) has the best performance when MMSE detection is present, as the CNB criterion minimizes the error in the MMSE receiver. Thus, by comparing the complexity and the performance of these relay selection algorithms and receivers, we recommend the use of MMD and ML detection, for $M_S \leq 2$ antennas, and CNB and linear MMSE detection, otherwise.

Appendix A
Proof of the Minimization of the PEP and of the Error in the ML Receiver - MMD

The ML detector is the optimal detector from the point of view of minimizing the probability of error (assuming equiprobable $\mathbf{x}$) and the solution is given by

$$\begin{aligned}\hat{\mathbf{x}}[i] &= \arg\min_{\mathbf{x}'[i]} \left(\left\| \mathbf{y}[i] - \sqrt{\frac{E_S}{M_S}} \mathbf{H}\mathbf{x}'[i] \right\|^2 \right), \\ &= \arg\min_{\mathbf{x}'[i]} \left(\left\| \sqrt{\frac{E_S}{M_S}} \mathbf{H}\mathbf{x}[i] + \mathbf{n}[i] - \sqrt{\frac{E_S}{M_S}} \mathbf{H}\mathbf{x}'[i] \right\|^2 \right).\end{aligned} \tag{40}$$

We have seen in Section IV that the PEP worst case is given by

$$\mathbf{P}(\mathbf{x}_n \to \mathbf{x}_l | \mathbf{H}) = Q\left(\sqrt{\frac{E_S}{2N_0 M_S} \mathcal{D}'_{min}} \right). \tag{41}$$

where $\mathcal{D}' = \|\mathbf{H}(\mathbf{x}_n - \mathbf{x}_l)\|^2$, in MA mode, and $\mathcal{D}' = \frac{1}{2}\|\mathbf{H}(\mathbf{x}_n - \mathbf{x}_l)\|^2$, in BC mode, and $l \neq n$.

The proposed MWC-Best-User-Link, using the MMD relay selection criterion, selects the channel matrix $\mathbf{H}^{MMD}$, minimizing the PEP worst case, as shown by

$$\begin{aligned}\mathbf{H}^{MMD} &= \arg\min_{\mathbf{H}} \mathbf{P}(\mathbf{x}_n \to \mathbf{x}_l|\mathbf{H}) \\ &= \arg\min_{\mathbf{H}} Q\left(\sqrt{\frac{E_S}{2N_0M_S}\mathcal{D}'_{min}}\right) \\ &= \arg\max_{\mathbf{H}} \left(\sqrt{\frac{E_S}{2N_0M_S}\mathcal{D}'_{min}}\right) \\ &= \arg\max_{\mathbf{H}} \mathcal{D}'_{min} \\ &= \arg\max_{\mathbf{H}} \min \|\mathbf{H}(\mathbf{x}_n - \mathbf{x}_l)\|^2 .\end{aligned} \tag{42}$$

Consequently, the MMD relay selection criterion, by maximizing the minimum Euclidian distance between different vectors of transmitted symbols, minimizes the error in the ML receiver, as shown by

$$\begin{aligned}\mathbf{H}^{MMD} &= \arg\max_{\mathbf{H}} \min \left(\left\|\sqrt{\frac{E_S}{M}}\mathbf{H}\mathbf{x}_n + \mathbf{n}[i] - \sqrt{\frac{E_S}{M}}\mathbf{H}\mathbf{x}_l\right\|^2\right) \\ &= \arg\max_{\mathbf{H}} \min \left(\frac{E_s}{M}\|\mathbf{H}\mathbf{x}_n - \mathbf{H}\mathbf{x}_l\|^2\right) \\ &= \arg\max_{\mathbf{H}} \min \|\mathbf{H}(\mathbf{x}_n - \mathbf{x}_l)\|^2 .\end{aligned} \tag{43}$$

This reasoning may be applied also for each of the square sub-matrices $\mathbf{H}^u$ in a non square matrix $\mathbf{H}$ (formed by multiple square sub-matrices). Thus, it is proven that the MMD relay selection criterion minimizes the error in the ML receiver, in the proposed MWC-Best-User-Link protocol.

APPENDIX B
PROOF OF THE SUM-RATE MAXIMIZATION - CNB

We have shown in Section IV that the sum-rate of a cooperative system in each time slot for a given channel matrix $\mathbf{H}$ is given by

$$\mathcal{R} = \frac{1}{2}\ \log_2 \det\left(\mathbf{H}(\mathbf{Q}/N_0)\mathbf{H}^H + \mathbf{I}\right), \tag{44}$$

where $\mathbf{Q} = E[\mathbf{x}(\mathbf{x})^H] = \mathbf{I}\ \frac{E_S}{M_S}$, in the MA mode, and $\mathbf{Q} = \mathbf{I}\ \frac{E_S}{2M_S}$, in BC mode. By considering a square channel matrix $\mathbf{H}$, the proposed MWC-Best-User-Link, using the CNB relay selection criterion, selects the channel matrix $\mathbf{H}^{CNB}$, maximizing the sum-rate, as shown by

$$\begin{aligned}\mathbf{H}^{CNB} &= \arg\max_{\mathbf{H}} \frac{1}{2}\ \log_2 \det\left(\mathbf{H}(\mathbf{Q}/N_0)\mathbf{H}^H + \mathbf{I}\right) \\ &= \arg\max_{\mathbf{H}} \det\left(\mathbf{H}(\mathbf{Q}/N_0)\mathbf{H}^H + \mathbf{I}\right) \\ &= \arg\max_{\mathbf{H}} \det\left(\mathbf{H}\mathbf{H}^H + \mathbf{I}\right) \\ &= \arg\max_{\mathbf{H}} \det\left(\mathbf{H}\mathbf{H}^H\right) \\ &= \arg\max_{\mathbf{H}} \det\left(\mathbf{H}\right)\det\left(\mathbf{H}^H\right) \\ &= \arg\max_{\mathbf{H}} \det\left(\mathbf{H}\right)\left(\det\left(\mathbf{H}\right)\right)' \\ &= \arg\max_{\mathbf{H}} \left|\det\left(\mathbf{H}\right)\right|^2 \\ &= \arg\max_{\mathbf{H}} \left|\det\left(\mathbf{H}\right)\right| .\end{aligned} \tag{45}$$

This reasoning may be applied also for each of the square sub-matrices $\mathbf{H}^u$ in a non square matrix $\mathbf{H}$ (formed by multiple square sub-matrices). Thus, it is proven that the CNB relay selection criterion maximizes the sum-rate in the proposed MWC-Best-User-Link protocol.

APPENDIX C
PROOF OF MINIMIZATION OF THE ERROR IN THE MMSE RECEIVER - CNB

In the linear MMSE receiver the estimate of the transmitted vector of symbols is given by

$$\begin{aligned}\tilde{\mathbf{x}}[i] &= \mathbf{W}_{\mathbf{MMSE}}\mathbf{y}[i] \\ &= \left(\mathbf{H}^H\mathbf{H} + \frac{\sigma_n^2}{\sigma_x^2}\mathbf{I}\right)^{-1}\mathbf{H}^H\mathbf{y}[i].\end{aligned} \tag{46}$$

Since $\mathbf{y}[i] = \mathbf{H}\mathbf{x}[i] + \mathbf{n}[i]$, from the above equation we can conclude that the performance of linear detection is directly related to the power of the MMSE effective noise [36] which is calculated as

$$E\left(\|\mathbf{n}_{\text{MMSE}}\|^2\right) = E\left(\left\|\left(\mathbf{H}^H\mathbf{H} + \frac{\sigma_n^2}{\sigma_x^2}\mathbf{I}\right)^{-1}\mathbf{H}^H\mathbf{n}[i]\right\|^2\right). \tag{47}$$

The effects of the effective noise in MMSE can be minimized if the power of the coefficients of the pseudo inverse channel matrix $\mathbf{W}_{ZF} = (\mathbf{H}^H\mathbf{H})^{-1}\mathbf{H}^H$ are small. Note that $\mathbf{W}_{ZF}$ corresponds to the equalization matrix in the Zero Forcing (ZF) receiver.

The relation between $\mathbf{W}_{ZF}$ and its determinant ($\det(\mathbf{W}_{ZF})$) is given by

$$\begin{aligned}\mathbf{W}_{ZF} &= (1/\det(\mathbf{W}_{ZF}^{-1}))\text{Adj}\left(\mathbf{W}_{ZF}^{-1}\right) \\ &= \det(\mathbf{W}_{ZF})\text{Adj}\left(\mathbf{W}_{ZF}^{-1}\right).\end{aligned} \tag{48}$$

By considering a square channel matrix $\mathbf{H}$, the proposed MWC-Best-User-Link, using the CNB relay selection criterion, selects the channel matrix $\mathbf{H}^{CNB}$, minimizing the effects

of the effective noise in ZF and MMSE receivers, as shown by

$$\begin{aligned}\mathbf{H}^{CNB} &= \arg\min_{\mathbf{H}} \det(\mathbf{W}_{\mathbf{ZF}}) \\ &= \arg\min_{\mathbf{H}} \det((\mathbf{H}^H\mathbf{H})^{-1}\mathbf{H}^H) \\ &= \arg\min_{\mathbf{H}} \left(\frac{\det\left(\mathbf{H}^H\right)}{\det\left(\mathbf{H}^H\mathbf{H}\right)}\right) \\ &= \arg\min_{\mathbf{H}} \left(\frac{\det\left(\mathbf{H}^H\right)}{\det(\mathbf{H}^H)\det(\mathbf{H})}\right) \\ &= \arg\min_{\mathbf{H}} \left(\frac{1}{\det(\mathbf{H})}\right) \\ &= \arg\max_{\mathbf{H}} \det(\mathbf{H}) = \arg\max_{\mathbf{H}} \left|\det\left(\mathbf{H}\right)\right|.\end{aligned} \tag{49}$$

This reasoning may be applied also for each of the square sub-matrices $\mathbf{H}^u$ in a non square matrix $\mathbf{H}$ (formed by multiple square sub-matrices). Thus, it is proven that the CNB relay selection criterion minimizes the error in ZF and, consequently, in the linear MMSE receiver, in the proposed MWC-Best-User-Link protocol.

REFERENCES

[1] J. N. Laneman; D. N. C. Tse; G. W. Wornell, "Cooperative Diversity in Wireless Networks: Efficient Protocols and Outage Behavior", in *IEEE Trans. Inf. Theory.*, vol. 50, no. 12, pp. 3062-3080, Dec. 2004.

[2] T. M. Cover, "Capacity Theorems for the Relay Channel", *IEEE Trans. Inf. Theory*, vol. 25, no. 5, pp. 572-584, Sept. 1979.

[3] D. Gündüz; A.Yener; A. Goldsmith; H. Poor, "The Multiway Relay Channel", in *IEEE Trans. Inf. Theory.*, vol. 59, no. 1, Jan. 2013.

[4] A. Ikhlef, D. S. Michalopoulos and R. Schober, "Max-Max Relay Selection for Relays with Buffers," in *IEEE Trans. Wireless Commun.*, vol. 11, no. 3, pp. 1124-1135, March 2012.

[5] T. Hesketh, R. C. De Lamare and S. Wales, "Joint maximum likelihood detection and link selection for cooperative MIMO relay systems," in *IET Commun.*, vol. 8, no. 14, pp. 2489-2499, Sept. 25 2014.

[6] P. Clarke and R. C. de Lamare, "Joint Transmit Diversity Optimization and Relay Selection for Multi-Relay Cooperative MIMO Systems Using Discrete Stochastic Algorithms," IEEE Communications Letters, vol. 15, no. 10, pp. 1035-1037, October 2011.

[7] P. Clarke and R. C. de Lamare, "Transmit Diversity and Relay Selection Algorithms for Multirelay Cooperative MIMO Systems," *IEEE Trans. Veh. Tech.*, vol. 61, no. 3, pp. 1084-1098, March 2012.

[8] Z. Zhang, Z. Ma, M. Xiao, G. K. Karagiannidis, Z. Ding and P. Fan, "Two-Timeslot Two-Way Full-Duplex Relaying for 5G Wireless Communication Networks," in *IEEE Trans. Commun.*, vol. 64, no. 7, pp. 2873-2887, July 2016.

[9] Ericsson, "5 G Radio Access", Ericsson White Paper, Uen 284 23-3204 Rev C | Apr. 2016 [Online]. Available: https://www.ericsson.com/assets/local/publications/white-papers/wp-5g.pdf.

[10] T. Q. S. Quek, M. Peng, O. Simeone, and W. Yu, Eds., "Cloud Radio Access Networks: Principles, Technologies, and Applications". Cambridge Univ. Press, Feb. 2017.

[11] I. Krikidis, "Relay Selection for Two-Way Relay Channels With MABC DF: A Diversity Perspective," in *IEEE Trans. Veh. Tech.*, vol. 59, no. 9, pp. 4620-4628, Nov. 2010.

[12] I. Krikidis, T. Charalambous, and J. Thompson, "Buffer-Aided Relay Selection for Cooperative Diversity Systems Without Delay Constraints", *IEEE Trans. Wireless Commun.*, vol. 11, no. 5, pp. 1957-1967, May 2012.

[13] J. Gu, R. C. de Lamare, "Joint interference cancellation and relay selection algorithms based on greedy techniques for cooperative DS-CDMA systems", Eurasip Journal on Wireless Communications and Networking, 2016, 59 (2016).

[14] J. Gu, R. C. de Lamare and M. Huemer, "Buffer-Aided Physical-Layer Network Coding With Optimal Linear Code Designs for Cooperative Networks," in *IEEE Trans. Commun.*, vol. 66, no. 6, pp. 2560-2575, June 2018.

[15] F. L. Duarte and R. C. de Lamare, "Buffer-Aided Max-Link Relay Selection for Multi-Way Cooperative Multi-Antenna Systems," in *IEEE Commun. Lett.*, vol. 23, no. 8, pp. 1423-1426, Aug. 2019.

[16] F. L. Duarte and R. C. de Lamare, "Cloud-Aided Multi-Way Multiple-Antenna Relaying with Best-User Link Selection and Joint ML Detection" in *24th International ITG Workshop on Smart Antennas (WSA 2020)*, Hamburg, Germany, 2020.

[17] F. L. Duarte and R. C. de Lamare, "Switched Max-Link Relay Selection Based on Maximum Minimum Distance for Cooperative MIMO Systems," *IEEE Trans. Veh. Tech.*, 2019.

[18] F. L. Duarte and R. C. de Lamare, "Buffer-Aided Max-Link Relay Selection for Two-Way Cooperative Multi-Antenna Systems", in *2019 16th Int. Symp. on Wireless Commun. Systems (ISWCS)*, Oulu, Finland, 2019, pp. 288-292.

[19] V. Jamali, N. Zlatanov and R. Schober, "Bidirectional Buffer-Aided Relay Networks With Fixed Rate Transmission—Part I: Delay-Unconstrained Case," in *IEEE Trans. Wireless Commun.*, vol. 14, no. 3, pp. 1323-1338, March 2015.

[20] V. Jamali, N. Zlatanov and R. Schober, "Bidirectional Buffer-Aided Relay Networks With Fixed Rate Transmission—Part II: Delay-Constrained Case," in *IEEE Trans. Wireless Commun.*, vol. 14, no. 3, pp. 1339-1355, March 2015.

[21] C. Wei, Z. Yin, W. Yang and Y. Cai, "Enhancing Physical Layer Security of DF Buffer-Aided Relay Networks With Small Buffer Sizes," in *IEEE Access*, vol. 7, pp. 128684-128693, 2019.

[22] G. Shabbir et al., "Buffer-Aided Successive Relay Selection Scheme for Energy Harvesting IoT Networks," in *IEEE Access*, vol. 7, pp. 36246-36258, 2019.

[23] A. Attarkashani, W. Hamouda, J. M. Moualeu and J. Haghighat, "Performance Analysis of Turbo Codes and Distributed Turbo Codes in Buffer-Aided Relay Systems," in *IEEE Trans. Commun.*, vol. 67, no. 7, pp. 4620-4633, July 2019.

[24] G. Liu, L. Li, L. J. Cimini and C. Shen, "Extending Proportional Fair Scheduling to Buffer-Aided Relay Access Networks," in *IEEE Trans. Veh. Tech.*, vol. 68, no. 1, pp. 1041-1044, Jan. 2019.

[25] S. M. Kim and M. Bengtsson, "Virtual full-duplex buffer-aided relaying in the presence of inter-relay interference," in *IEEE Trans. Wireless Commun.*, vol. 15, no. 4, pp. 2966-2980, April 2016.

[26] T. Charalambous, S. M. Kim, N. Nomikos, M. Bengtsson, M. Johansson, "Relay-pair selection in buffer-aided successive opportunistic relaying using a multi-antenna source," in *Ad Hoc Netw.*, vol. 84, pp. 29-41, 2019.

[27] C. Wei, W. Yang, Y. Cai, X. Tang and G. Kang, "Secrecy Outage Performance for DF Buffer-Aided Relaying Networks With a Multi-Antenna Destination," in *IEEE Access*, vol. 7, pp. 41349-41364, 2019.

[28] H. Liu, P. Popovski, E. d. Carvalho and Y. Zhao, "Sum-Rate Optimization in a Two-Way Relay Network with Buffering," in *IEEE Commun. Lett.*, vol. 17, no. 1, pp. 95-98, Jan. 2013.

[29] S. Zhang and S. C. Liew, "Applying Physical-layer Network Coding in Wireless Networks, *Eurasip Journal of Wireless Commun. and Netw.*, 2010.

[30] R. K. Ahiadormey, P. Anokye, H. Jo and K. Lee, "Performance Analysis of Two-Way Relaying in Cooperative Power Line Communications," in *IEEE Access*, vol. 7, pp. 97264-97280, 2019.

[31] F. Engel, T. Abrão and L. Hanzo, "Relay selection methods for maximizing the lifetime of wireless sensor networks," 2013 *IEEE Wireless Commun. and Netw. Conf. (WCNC)*, Shanghai, 2013, pp. 2339-2344.

[32] "Mimo Detection Algorithms" , November 2017 [Online]. Available: https://web.stanford.edu/class/ee359/pdfs/mimo-detection-algorithms.pdf

[33] H. Joudeh and B. Clerckx, "Sum-Rate Maximization for Linearly Precoded Downlink Multiuser MISO Systems With Partial CSIT: A Rate-Splitting Approach," in *IEEE Trans. Commun.*, vol. 64, no. 11, pp. 4847-4861, Nov. 2016.

[34] D. Poulimeneas, T. Charalambous, N. Nomikos, I. Krikidis, D. Vouyioukas and M. Johansson, "Delay- and diversity-aware buffer-aided relay selection policies in cooperative networks," *2016 IEEE Wireless Commun. and Netw. Conf., Doha, 2016*, pp. 1-6.

[35] Z. Tian, G. Chen, Y. Gong, Z. Chen, and J. Chambers, "Buffer-Aided Max-Link Relay Selection in Amplify-and-Forward Cooperative Networks," *IEEE Trans. Veh. Tech.*, vol. 64, no. 2, pp. 553–565, Feb. 2015.

[36] P. Li, R. C. de Lamare and R. Fa, "Multiple Feedback Successive Interference Cancellation Detection for Multiuser MIMO Systems," in *IEEE Trans. Wireless Commun.*, vol. 10, no. 8, pp. 2434-2439, Aug. 2011.

[37] I. E. Telatar, "Capacity of multi-antenna gaussian channels" *AT&T Bell Laboratories, Internal Tech. Memo*, June 1995.

[38] R. C. de Lamare, "Massive MIMO systems: Signal processing challenges and future trends," in URSI Radio Science Bulletin, vol. 2013, no. 347, pp. 8-20, Dec. 2013.

[39] W. Zhang et al., "Large-Scale Antenna Systems With UL/DL Hardware Mismatch: Achievable Rates Analysis and Calibration," in IEEE Transactions on Communications, vol. 63, no. 4, pp. 1216-1229, April 2015.

[40] R. C. de Lamare and R. Sampaio-Neto, "Adaptive MBER decision feedback multiuser receivers in frequency selective fading channels," in IEEE Communications Letters, vol. 7, no. 2, pp. 73-75, Feb. 2003.

[41] R. C. De Lamare, R. Sampaio-Neto and A. Hjorungnes, "Joint iterative interference cancellation and parameter estimation for cdma systems," in IEEE Communications Letters, vol. 11, no. 12, pp. 916-918, December 2007.

[42] R. C. De Lamare and R. Sampaio-Neto, "Minimum Mean-Squared Error Iterative Successive Parallel Arbitrated Decision Feedback Detectors for DS-CDMA Systems," in IEEE Transactions on Communications, vol. 56, no. 5, pp. 778-789, May 2008.

[43] Y. Cai and R. C. de Lamare, "Space-Time Adaptive MMSE Multiuser Decision Feedback Detectors With Multiple-Feedback Interference Cancellation for CDMA Systems," in IEEE Transactions on Vehicular Technology, vol. 58, no. 8, pp. 4129-4140, Oct. 2009.

[44] R. C. de Lamare and R. Sampaio-Neto, "Adaptive Reduced-Rank Equalization Algorithms Based on Alternating Optimization Design Techniques for MIMO Systems," in IEEE Transactions on Vehicular Technology, vol. 60, no. 6, pp. 2482-2494, July 2011.

[45] P. Li, R. C. de Lamare and R. Fa, "Multiple Feedback Successive Interference Cancellation Detection for Multiuser MIMO Systems," in IEEE Trans. on Wireless Comm., vol. 10, no. 8, pp. 2434-2439, Aug. 2011.

[46] N. Song, R. C. de Lamare, M. Haardt and M. Wolf, "Adaptive Widely Linear Reduced-Rank Interference Suppression Based on the Multistage Wiener Filter," in IEEE Transactions on Signal Processing, vol. 60, no. 8, pp. 4003-4016, Aug. 2012.

[47] P. Li and R. C. De Lamare, "Adaptive Decision-Feedback Detection With Constellation Constraints for MIMO Systems," in IEEE Transactions on Vehicular Technology, vol. 61, no. 2, pp. 853-859, Feb. 2012.

[48] R. C. de Lamare, "Adaptive and Iterative Multi-Branch MMSE Decision Feedback Detection Algorithms for Multi-Antenna Systems," in IEEE Transactions on Wireless Communications, vol. 12, no. 10, pp. 5294-5308, October 2013.

[49] P. Li and R. C. de Lamare, "Distributed Iterative Detection With Reduced Message Passing for Networked MIMO Cellular Systems," in IEEE Transactions on Vehicular Technology, vol. 63, no. 6, pp. 2947-2954, July 2014.

[50] Y. Cai, R. C. de Lamare, B. Champagne, B. Qin and M. Zhao, "Adaptive Reduced-Rank Receive Processing Based on Minimum Symbol-Error-Rate Criterion for Large-Scale Multiple-Antenna Systems," in IEEE Transactions on Communications, vol. 63, no. 11, pp. 4185-4201, Nov. 2015.

[51] H. Ruan and R. C. de Lamare, "Robust Adaptive Beamforming Using a Low-Complexity Shrinkage-Based Mismatch Estimation Algorithm," *IEEE Signal Processing Letters*, vol. 21, no. 1, pp. 60-64, Jan. 2014.

[52] H. Ruan and R. C. de Lamare, "Robust Adaptive Beamforming Based on Low-Rank and Cross-Correlation Techniques," *IEEE Transactions on Signal Processing*, vol. 64, no. 15, pp. 3919-3932, 1 Aug.1, 2016.

[53] H. Ruan and R. C. de Lamare, "Distributed Robust Beamforming Based on Low-Rank and Cross-Correlation Techniques: Design and Analysis," in IEEE Transactions on Signal Processing, vol. 67, no. 24, pp. 6411-6423, 15 Dec.15, 2019.

[54] N. Song, W. U. Alokozai, R. C. de Lamare and M. Haardt, "Adaptive Widely Linear Reduced-Rank Beamforming Based on Joint Iterative Optimization," in IEEE Signal Processing Letters, vol. 21, no. 3, pp. 265-269, March 2014.

[55] A. G. D. Uchoa, C. T. Healy and R. C. de Lamare, "Iterative Detection and Decoding Algorithms for MIMO Systems in Block-Fading Channels Using LDPC Codes," in IEEE Transactions on Vehicular Technology, vol. 65, no. 4, pp. 2735-2741, April 2016.

[56] Z. Shao, R. C. de Lamare and L. T. N. Landau, "Iterative Detection and Decoding for Large-Scale Multiple-Antenna Systems With 1-Bit ADCs," in IEEE Wireless Communications Letters, vol. 7, no. 3, pp. 476-479, June 2018.

[57] R. B. Di Renna and R. C. de Lamare, "Adaptive Activity-Aware Iterative Detection for Massive Machine-Type Communications," in IEEE Wireless Communications Letters, vol. 8, no. 6, pp. 1631-1634, Dec. 2019.

[58] K. Zu and R. C. de Lamare, "Low-Complexity Lattice Reduction-Aided Regularized Block Diagonalization for MU-MIMO Systems," in IEEE Communications Letters, vol. 16, no. 6, pp. 925-928, June 2012.

[59] Y. Cai, R. C. de Lamare, and R. Fa, "Switched Interleaving Techniques with Limited Feedback for Interference Mitigation in DS-CDMA Systems," IEEE Transactions on Communications, vol.59, no.7, pp.1946-1956, July 2011.

[60] Y. Cai, R. C. de Lamare, D. Le Ruyet, "Transmit Processing Techniques Based on Switched Interleaving and Limited Feedback for Interference Mitigation in Multiantenna MC-CDMA Systems," IEEE Transactions on Vehicular Technology, vol.60, no.4, pp.1559-1570, May 2011.

[61] K. Zu, R. C. de Lamare and M. Haardt, "Generalized Design of Low-Complexity Block Diagonalization Type Precoding Algorithms for Multiuser MIMO Systems," IEEE Transactions on Communications, vol. 61, no. 10, pp. 4232-4242, October 2013.

[62] W. Zhang et al., "Widely Linear Precoding for Large-Scale MIMO with IQI: Algorithms and Performance Analysis," IEEE Transactions on Wireless Communications, vol. 16, no. 5, pp. 3298-3312, May 2017.

[63] K. Zu, R. C. de Lamare and M. Haardt, "Multi-Branch Tomlinson-Harashima Precoding Design for MU-MIMO Systems: Theory and Algorithms," IEEE Transactions on Communications, vol. 62, no. 3, pp. 939-951, March 2014.

[64] L. Zhang, Y. Cai, R. C. de Lamare and M. Zhao, "Robust Multibranch Tomlinson-Harashima Precoding Design in Amplify-and-Forward MIMO Relay Systems," IEEE Transactions on Communications, vol. 62, no. 10, pp. 3476-3490, Oct. 2014.

[65] L. T. N. Landau and R. C. de Lamare, "Branch-and-Bound Precoding for Multiuser MIMO Systems With 1-Bit Quantization," in IEEE Wireless Communications Letters, vol. 6, no. 6, pp. 770-773, Dec. 2017.

[66] L. T. N. Landau, M. Dorpinghaus, R. C. de Lamare and G. P. Fettweis, "Achievable Rate With 1-Bit Quantization and Oversampling Using Continuous Phase Modulation-Based Sequences," in IEEE Transactions on Wireless Communications, vol. 17, no. 10, pp. 7080-7095, Oct. 2018.

[67] A. R. Flores, R. C. de Lamare and B. Clerckx, "Linear Precoding and Stream Combining for Rate Splitting in Multiuser MIMO Systems," in IEEE Communications Letters, vol. 24, no. 4, pp. 890-894, April 2020.

[68] T. Wang, R. C. de Lamare, and P. D. Mitchell, "Low-Complexity Set-Membership Channel Estimation for Cooperative Wireless Sensor Networks," IEEE Transactions on Vehicular Technology, vol.60, no.6, pp.2594-2607, July 2011.

[69] T. Wang, R. C. de Lamare and A. Schmeink, "Joint linear receiver design and power allocation using alternating optimization algorithms for wireless sensor networks," *IEEE Trans. on Vehi. Tech.*, vol. 61, pp. 4129-4141, 2012.

[70] R. C. de Lamare, "Joint iterative power allocation and linear interference suppression algorithms for cooperative DS-CDMA networks", IET Communications, vol. 6, no. 13 , 2012, pp. 1930-1942.

[71] T. Peng, R. C. de Lamare and A. Schmeink, "Adaptive Distributed Space-Time Coding Based on Adjustable Code Matrices for Cooperative MIMO Relaying Systems", *IEEE Transactions on Communications*, vol. 61, no. 7, July 2013.

[72] T. Peng and R. C. de Lamare, "Adaptive Buffer-Aided Distributed Space-Time Coding for Cooperative Wireless Networks," *IEEE Transactions on Communications*, vol. 64, no. 5, pp. 1888-1900, May 2016.

[73] J. Gu, R. C. de Lamare and M. Huemer, "Buffer-Aided Physical-Layer Network Coding with Optimal Linear Code Designs for Cooperative Networks," *IEEE Transactions on Communications*, 2018.

[74] C. T. Healy and R. C. de Lamare, "Design of LDPC Codes Based on Multipath EMD Strategies for Progressive Edge Growth," *IEEE Transactions on Communications*, vol. 64, no. 8, pp. 3208-3219, Aug. 2016.

[75] M. L. Honig and J. S. Goldstein, "Adaptive reduced-rank interference suppression based on the multistage Wiener filter," *IEEE Transactions on Communications*, vol. 50, no. 6, June 2002.

[76] Q. Haoli and S.N. Batalama, "Data record-based criteria for the selection of an auxiliary vector estimator of the MMSE/MVDR filter", *IEEE Transactions on Communications*, vol. 51, no. 10, Oct. 2003, pp. 1700 - 1708.

[77] R. C. de Lamare and R. Sampaio-Neto, "Reduced-Rank Adaptive Filtering Based on Joint Iterative Optimization of Adaptive Filters", *IEEE Signal Processing Letters*, Vol. 14, no. 12, December 2007.

[78] R. C. de Lamare and R. Sampaio-Neto, "Adaptive Reduced-Rank Processing Based on Joint and Iterative Interpolation, Decimation and Filtering", *IEEE Transactions on Signal Processing*, vol. 57, no. 7, July 2009, pp. 2503 - 2514.

[79] R. C. de Lamare and R. Sampaio-Neto, "Reduced-rank space-time adaptive interference suppression with joint iterative least squares algorithms

for spread-spectrum systems," *IEEE Trans. Vehi. Technol.*, vol. 59, no. 3, pp. 1217-1228, Mar. 2010.

[80] R. C. de Lamare and R. Sampaio-Neto, "Adaptive reduced-rank equalization algorithms based on alternating optimization design techniques for MIMO systems," *IEEE Trans. Vehi. Technol.*, vol. 60, no. 6, pp. 2482-2494, Jul. 2011.

[81] S. Xu, R. C. de Lamare and H. V. Poor, "Distributed Compressed Estimation Based on Compressive Sensing," *IEEE Signal Processing Letters*, vol. 22, no. 9, pp. 1311-1315, Sept. 2015.

[82] Y. Jiang et al., "Joint Power and Bandwidth Allocation for Energy-Efficient Heterogeneous Cellular Networks," in IEEE Transactions on Communications, vol. 67, no. 9, pp. 6168-6178, Sept. 2019.

[83] F. L. Duarte and R. C. De Lamare, "Cloud-Driven Multi-Way Multiple-Antenna Relay Systems: Joint Detection, Best-User-Link Selection and Analysis," IEEE Transactions on Communications, 2020.